

Sus1 maintains a normal lifespan through regulation of TREX-2 complex-mediated mRNA export

Suji Lim^{1,*}, Yan Liu^{1,*}, Byung-Ho Rhie¹, Chun Kim¹, Hong-Yeoul Ryu^{2,#}, Seong Hoon Ahn^{1,#}

¹Department of Molecular and Life Science, College of Science and Convergence Technology, Hanyang University, Ansan, Gyeonggi-do 15588, Republic of Korea

²BK21 Plus KNU Creative BioResearch Group, School of Life Sciences, College of National Sciences, Kyungpook National University, Daegu 41566, Republic of Korea

*Equal contribution

#Jointly supervised the study

Correspondence to: Hong-Yeoul Ryu, Seong Hoon Ahn; **email:** rhr4757@knu.ac.kr, hoon320@hanyang.ac.kr

Keywords: Sus1, SAGA DUB module, TREX-2, replicative lifespan, mRNA export

Received: April 1, 2022

Accepted: June 14, 2022

Published: June 29, 2022

Copyright: © 2022 Lim et al. This is an open access article distributed under the terms of the [Creative Commons Attribution License](https://creativecommons.org/licenses/by/3.0/) (CC BY 3.0), which permits unrestricted use, distribution, and reproduction in any medium, provided the original author and source are credited.

ABSTRACT

Eukaryotic gene expression requires multiple cellular events, including transcription and RNA processing and transport. Sus1, a common subunit in both the Spt-Ada-Gcn5 acetyltransferase (SAGA) and transcription and export complex-2 (TREX-2) complexes, is a key factor in coupling transcription activation to mRNA nuclear export. Here, we report that the SAGA DUB module and TREX-2 distinctly regulate yeast replicative lifespan in a Sir2-dependent and -independent manner, respectively. The growth and lifespan impaired by *SUS1* loss depend on TREX-2 but not on the SAGA DUB module. Notably, an increased dose of the mRNA export factors Mex67 and Dbp5 rescues the growth defect, shortened lifespan, and nuclear accumulation of poly(A)⁺ RNA in *sus1Δ* cells, suggesting that boosting the mRNA export process restores the mRNA transport defect and the growth and lifespan damage in *sus1Δ* cells. Moreover, Sus1 is required for the proper association of Mex67 and Dbp5 with the nuclear rim. Together, these data indicate that Sus1 links transcription and mRNA nuclear export to the lifespan control pathway, suggesting that prevention of an abnormal accumulation of nuclear RNA is necessary for maintenance of a normal lifespan.

INTRODUCTION

Aging is a process accompanied by the gradual accumulation of molecular, cellular, and organ damage during sexual maturity, eventually leading to the decay of biological functions and increased vulnerability to morbidity and mortality [1, 2]. The budding yeast *Saccharomyces cerevisiae* is a useful model organism for studying the aging process, and this model is analyzed through two distinct methods: replicative lifespan (RLS) and chronological lifespan (CLS) [3]. The RLS assay monitors how many daughter cells can be produced from a mother cell to study the lifespan of proliferating cells, such as stem cells, whereas CLS is a

model of the aging process of postmitotic cells in multicellular organisms by measuring how long a cell can survive in a nondividing state.

Lifespan studies using the yeast model system have revealed diverse conserved genetic pathways that influence aging, such as the Sir2 histone deacetylase-mediated maintenance of intact telomeric chromatin or suppression of rDNA recombination [4–7]. Among such factors involved in lifespan control, the Spt-Ada-Gcn5 acetyltransferase (SAGA) transcription coactivator complex, which has recently been identified as a regulator of the aging pathway, has multiple roles in the yeast lifespan. SAGA consists of four functionally

independent modules: the HAT module (histone acetylation), DUB module (deubiquitination of H2B), TAF module (coactivator architecture), and SPT module (assembly of the preinitiation complex) [8]. RLS is extended by the presence of a HAT inhibitor, inducing a similar effect as Sir2 activation, and is completely abolished by the loss of Gcn5, a subunit of the SAGA HAT module [9]. Furthermore, the heterozygous *GCN5* mutant or *NGG1* (a linker protein between Gcn5 and SAGA [10]) mutant, exhibits an increase in RLS [9]. However, yeast cells entirely lacking each component in the SAGA HAT module either do not exhibit an extended lifespan or show a decreased lifespan [11, 12]. Loss of Ubp8, Sgf73, or Sgf11 in the SAGA DUB module exceptionally extends RLS in a Sir2-dependent manner by enhancing telomeric silencing and promoting rDNA stability [11], whereas absence of the components in the SAGA SPT module mostly leads to a decrease in both RLS and CLS [12]. In particular, Spt7 in the SAGA SPT module is indispensable for a normal lifespan by maintaining genome stability and overall mRNA expression and is independent of Sir2 [12]. In addition, SAGA facilitates the retention and accumulation of extrachromosomal DNA circles and anchoring of the DNA circle molecules to the nuclear pore complex (NPC), causing the organization of aged nuclei [13]. Although it is still uncertain how a single complex has multiple roles to ensure a normal lifespan, this is a good example of how aging is finely tuned by an intricate network of regulators.

SAGA interacts functionally and physically with the transcription and export complex-2 (TREX-2) complex composed of Sac3, Thp1, Cdc31, Sem1, and Sus1. This link is important for the transcription, mRNA export, and targeting of active genes to the NPC [14]. The N-terminus in Sac3 provides a platform for association with Thp1 and Sem1 to form an mRNA-binding module and for association with the essential mRNA exporter Mex67, whereas its C-terminus binds to Sus1, Cdc31, and the Nup1 nucleoporin, providing attachment of the complex to the NPC [15–19]. TREX-2 shares one subunit, Sus1, with the SAGA DUB module, and Sus1 is also found at the promoter and coding regions in some SAGA-dependent genes, contributing to the coupling of transcription activation and mRNA export [20–23]. In particular, Sus1, Sac3, and Thp1 mediate the proper tethering of transcribed genes to NPCs upon the activation of transcription [24–26]. Both Cdc31 and Sem1 also contribute to promoting the association of TREX-2 with the NPC and mRNA export [17, 27].

In eukaryotes, NPCs, composed of ~30 nucleoporin proteins, maintain a nuclear permeability barrier that selectively allows small molecules to diffuse in and out

of the nucleus [28]. Approximately half of the nucleoporins have characteristic domains with FG-repeat motifs, such as FG, FXFG, and GLFG. These FG domains are required for targeting nuclear membrane proteins, the permeability barrier, and chromatin association with NPCs [29]. Age-dependent oxidative damage to nucleoporins disrupts the structure and function of NPCs in postmitotic cells, leading to leakage of cytoplasmic proteins into the nucleus [30]. In entirely differentiated rat brain cells, nucleoporins are oxidized and long-lived without degradation or replacement with newly synthesized proteins, with potentially harmful implications [30, 31]. Yeast RLS experiments provide more direct evidence of a correlation between NPCs and cellular lifespans [32]. Yeast cells lacking the GLFG domain of Nup116 exhibit a decrease in RLS. This shortened lifespan depends on Kap121-mediated defects in nuclear transport, which disrupt mitochondrial activity. In contrast, the Nup100-mediated nuclear export of specific tRNAs potentially limits yeast lifespan [32, 33].

Here, we report that loss of *SUS1* triggers slow growth and a shortened lifespan in yeast cells. Although Sus1 certainly belongs to both the SAGA DUB module and TREX-2, cellular propagation and replicative ability impaired by *SUS1* loss are not altered by the additional deletion of the TREX-2 subunit, *sac3* or *thp1* but not the SAGA DUB module, suggesting that Sus1 is involved in the regulation of lifespan in a TREX-2-dependent manner. Additionally, unlike the SAGA DUB module, TREX-2-mediated lifespan control is independent of the presence of Sir2. Using a tiled yeast genomic DNA library, we found that overexpression of either Mex67 or Dbp5, mRNA export factors, suppresses growth defects in *sus1Δ* cells. Consistent with this result, the decreased RLS and nuclear accumulation of poly(A)⁺ RNA upon the lack of *SUS1* were rescued by an increased dose of Mex67 or Dbp5. Furthermore, Dbp5 mislocalization at the nuclear rim is greatly increased in *sus1Δ* cells. Taken together, these data suggest that Sus1 links transcription and mRNA nuclear export to the lifespan control pathway, indicating that blocking abnormal accumulation of nuclear RNA is required for maintaining a normal lifespan.

RESULTS

Deficient *sus1* allele results in the shortening of lifespan

Despite diverse attempts to define the correlation between the SAGA DUB module and yeast lifespan, the function of Sus1 in the lifespan remains elusive [11]. To investigate the role of Sus1 in the control of yeast

lifespan, we first analyzed the yeast RLS of 50 cells from four independent *sus1Δ* strains, which exhibit a comparable slow growth phenotype between strains (Figure 1A and 1B). Although McCormick and colleagues previously reported that loss of Sus1 had no effect on lifespan when the replicative ability of 40 yeast cells was examined by micromanipulation [11], we observed that the mean lifespans of all four independent *sus1Δ* strains were equally shorter than that of wild-type (WT) to a similar degree. The different results between the two studies are likely derived from the increased number of cells and bioreplicates in our study. These observations provide the first evidence that Sus1 is required for a normal cellular lifespan.

The SAGA DUB module and TREX-2 differentially affect lifespan

Sus1 is a component of the evolutionarily conserved SAGA DUB module and TREX-2 coupling of histone H2B deubiquitination-mediated transcriptional activation to nuclear pore-associated mRNA export [20, 21, 34]. Therefore, we next examined the change in RLS caused by the absence of nonessential genes encoding the individual subunits of the SAGA DUB module and TREX-2 (Figure 1C and 1D). Consistent with previous results [11], we observed exceptionally long-lived *ubp8Δ* and *sgf73Δ* strains and only a mild increase in the lifespan of the *sgf11Δ* strain, whereas the lack of these genes did not affect yeast cell growth (Figure 1C and 1E). In contrast, interestingly, loss of the two major structural components of TREX-2, Thp1 and

Sac3, but not Sem1, impaired normal lifespan and vegetative growth at different temperatures more strongly than the lack of the linker protein Sus1 between the SAGA DUB module and TREX-2 (Figure 1D and 1E). Taken together, these results indicate that the SAGA DUB module and TREX-2 distinctly affect cellular growth and lifespan, and the effects of their common subunit Sus1 correspond with those of TREX-2 but not the SAGA DUB module.

Sus1 affects lifespan independently of other subunits in the SAGA DUB module

SAGA and TREX-2 complexes are physically and functionally linked, whereas their impact on lifespan is clearly distinguished (Figure 1C–1E). Therefore, we next sought to determine which complex-dependent pathways are responsible for the shortened lifespan caused by loss of Sus1 (Figure 2). Sus1 is necessary for the association of Ubp8 and Sgf11 with the main body of SAGA, resulting in balanced H2B ubiquitination levels [21]. If a decreased lifespan in *sus1Δ* cells is exclusively due to the effects of the SAGA DUB module, Sus1 loss will not shorten the lifespan in the *ubp8Δ*, *sgf11Δ*, and *sgf73Δ* backgrounds. However, the extended RLS of the *ubp8Δ*, *sgf11Δ*, and *sgf73Δ* strains was significantly suppressed by the additional deletion of *SUS1*, indicating that Sus1 influences RLS through perhaps other function(s) with H2B deubiquitination activity in the SAGA (Figure 2A–2C). Furthermore, the slow growth phenotype and the heat and cold sensitivities of the *sus1Δ* strain were not affected by the

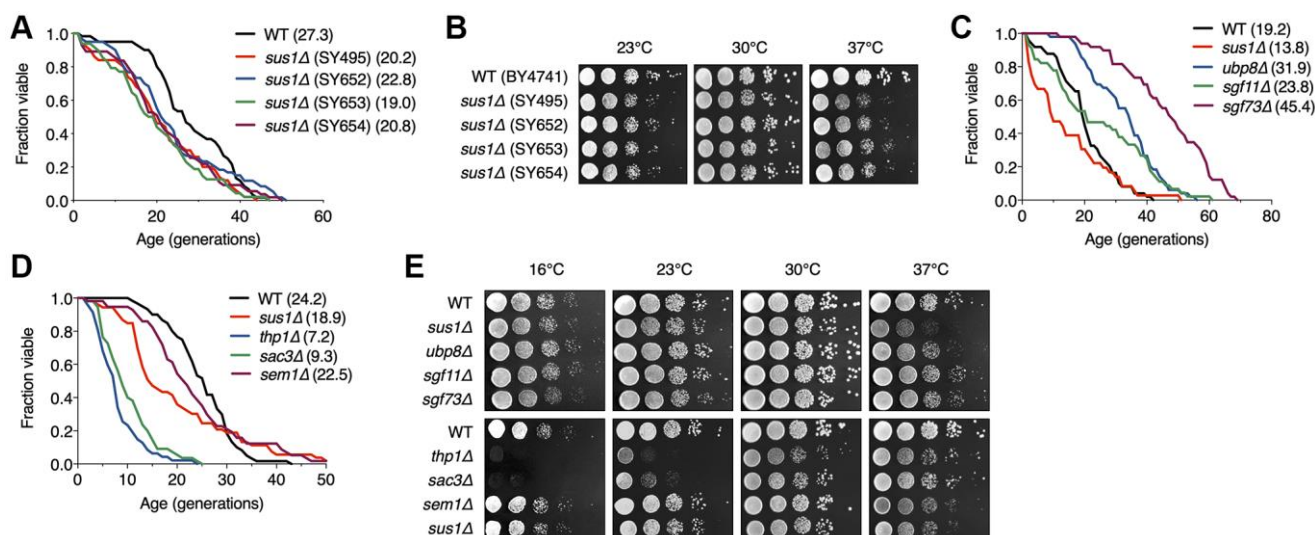


Figure 1. RLS is shortened by the loss of Sus1. (A) RLS analysis of four independent *sus1Δ* strains. The *SUS1* allele was replaced with *HISMX6* in SY495 and SY652 and *KanMX6* in SY653 and SY654. The mean lifespans are shown in parentheses. (B) Growth analysis of the strains used in (C). After spotting cells in 10-fold serial dilutions, the YPD plates were incubated at the indicated temperatures for 2–3 days. (C and D) RLS analysis of the indicated mutants of the SAGA DUB module (C) and TREX-2 (D). The mean lifespans are shown in parentheses. (E) Growth analysis of the strains used in (C and D). After spotting cells in 10-fold serial dilutions, the YPD plates were incubated for 2–3 days at 23°C, 30°C, and 37°C and for 5 days at 16°C.

additional deletion of *UBP8* or *SGF73*, although there was a mild increase in cold sensitivity in the *sus1Δ sgf11Δ* double mutant (Figure 2G). Overall, these data suggest that Sus1 contributes to the control of lifespan independent of the SAGA DUB module-mediated pathway.

Sus1 regulates lifespan through the TREX-2-dependent pathway

We next investigated whether Sus1-dependent lifespan shortening is determined by a TREX-2-driven pathway. Interestingly, additional *SUS1* loss did not affect the

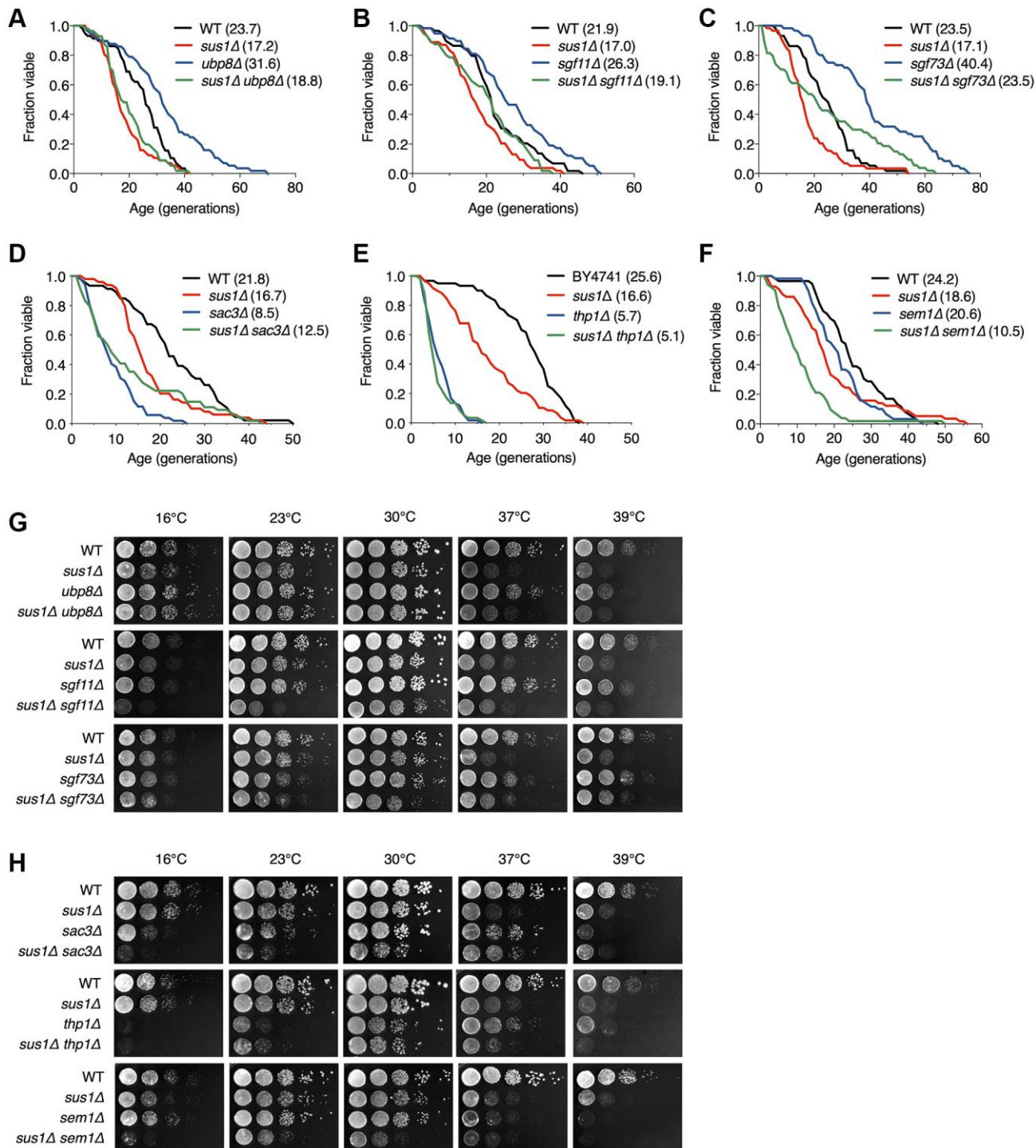


Figure 2. Additional mutations of TREX-2 components enhance the RLS and growth defects in *sus1Δ* strains. (A–F) RLS analysis of the indicated mutants. The mean lifespans are shown in parentheses. (G and H) Growth analysis of the strains used in (A–F), as described in Figure 1E.

shortened lifespan in *sac3Δ* and *thp1Δ*, indicating that the effects of Sus1 on RLS rely on the presence of Sac3 and Thp1, which functions as a platform that mediates chromatin binding of TREX-2 (Figure 2D and 2E). RLS in the *sem1* mutant was indistinguishable from that in WT cells (Figure 1D). However, the altered lifespan of the *sus1Δ sem1Δ* double mutant significantly exceeded that of either single mutant, suggesting an additive effect on the lifespan as a result of the combined deletion of *SUS1* and *SEMI* (Figure 2F). Although Sus1 and Sem1 are not the main and essential subunits of TREX-2, they effectively support TREX-2-mediated mRNP biogenesis and mRNA export [27, 34, 35]. Therefore, this result indicated that the loss of both *SUS1* and *SEMI* boosts the suppression of TREX-2 activity. In contrast to the growth analysis results in *sus1Δ ubp8Δ* and *sus1Δ sgf11Δ* strains (Figure 2G), the slow growth and the heat, cold, and hydroxyurea (HU) sensitivities of *sus1Δ* cells were more significantly impaired by the additional loss of genes encoding the TREX-2 components *SAC3*, *THP1*, or *SEMI*, suggesting that Sus1 is an important

factor for TREX-2 activity (Figure 2H and Supplementary Figure 1). Taken together, these results strongly suggested that Sus1 is necessary for normal cellular lifespan through a pathway dependent on TREX-2 but not the SAGA DUB module.

TREX-2 functions in a Sir2-independent pathway

We next addressed how TREX-2 is involved in lifespan regulation. Because Sir2 is a well-known factor that modulates RLS [4, 6, 36], we subsequently investigated whether Sir2 affects RLS in TREX-2 mutants. The SAGA DUB module, including Sus1, was previously reported to control RLS via interaction with Sir2 [11]. As expected, we also observed that the extended lifespan in *ubp8Δ* and *sgf73Δ* strains failed due to the deletion of another gene (*SIR2*; Figure 3A). In addition, a similar result was found in *sir2Δ sgf11Δ* cells, which also failed to show an increase in lifespan in the absence of Sgf11. However, although the degree of RLS decrease was similar between *sir2Δ* and *sir2Δ sus1Δ*

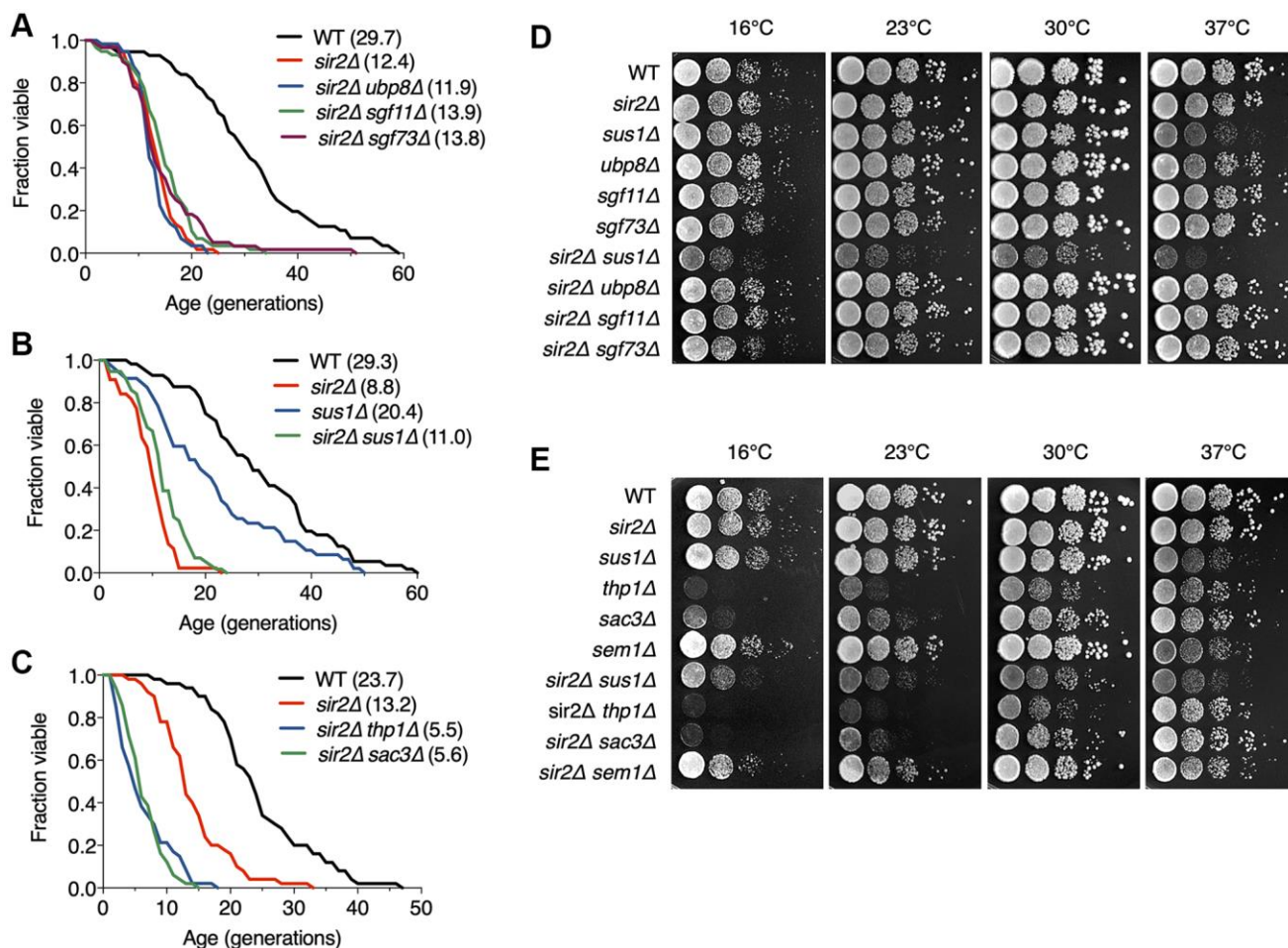


Figure 3. TREX-2 affects RLS in a Sir2-independent manner. (A–C) RLS analysis of double deletion strains of SAGA DUB mutants (A), *sus1Δ* mutants (B) and TREX-2 mutants (C) in combination with *sir2Δ*. The mean lifespans are shown in parentheses. (D and E) Growth analysis of the strains used in (A–C), as described in Figure 1E.

cells (Figure 3B), the absence of Thp1 or Sac3 more significantly impaired the shortened lifespan of *sir2Δ* cells (Figure 3C), suggesting that TREX-2 has a role in lifespan modulation via a Sir2-independent mechanism. Because *sus1* deletion has a milder effect on RLS than *thp1* or *sac3* mutations (Figure 1D), Sus1 might marginally affect a change in the lifespan of the *sir2Δ* strain.

The silencing function of Sir2 contributes to extending RLS by suppressing rDNA recombination [4]. Nevertheless, in contrast with the lack of Ubp8, loss of Sus1 affected neither silencing nor recombination at the rDNA loci (Supplementary Figure 2). Instead, *SIR2* loss significantly impaired the growth of *sus1Δ* cells, whereas Sir2 did not affect the growth of mutants of other components in the SAGA DUB module or TREX-2 (Figure 3D and 3E), suggesting that Sus1 influences yeast cell growth via a Sir2-independent pathway.

Taken together, these data indicate that the SAGA DUB module and TREX-2 are required for lifespan regulation through distinct cellular mechanisms. In particular, this finding reveals a novel Sir2-independent pathway that sustains RLS, perhaps through TREX-2 activity.

Overexpression of the nuclear RNA export factors Mex67 and Dbp5 rescues the lifespan defect in *sus1Δ* cells

TREX-2 associates not only with SAGA but also with the NPC basket structure, and its ability to interact with multiple factors contributes to establishing the link between transcription, pre-mRNA processing, and mRNA export [37]. Age-dependent deterioration of NPCs leads to loss of the nuclear permeability barrier, causing defects in nuclear integrity [30]. Each FG nucleoporin, an intrinsically disordered regulator of nucleocytoplasmic transport, in NPCs distinctly affects aging, whereas Nup100 loss shows increased lifespan, and longevity is impaired in *nup16* mutants [32, 33].

To determine whether the TREX-2-mediated lifespan regulation pathway is related to the role of NPCs in the aging control mechanism, we screened for NPC genes that prevent a defect in cell growth, which is usually positively related to RLS, upon *SUS1* deletion (Figure 4B and Supplementary Figure 3). To monitor cell proliferation immediately after a *SUS1* gene was lost, we used a strain carrying the *sus1Δ* allele in the chromosome and a covering WT *SUS1* plasmid that could be readily evicted in 5-FOA medium; the *URA3* gene product is toxic to cells cultured on 5-FOA (Figure 4A). The WT strain (*sus1Δ* + p*SUS1*) was then transformed with 46 different library plasmids containing individual NPC genes and proteins known to

physically interact with NPCs, searched in the *Saccharomyces* Genome Database (SGD; <https://www.yeastgenome.org>), and yeast cell growth was measured after eviction of the *SUS1* cover plasmid (Figure 4B and Supplementary Figure 3). Transformants expressing a library plasmid, including Asm4, an FG nucleoporin component of the central core of the NPC [38], displayed a more severe growth defect than the null *sus1* mutant, suggesting cooperation between TREX-2 and the previously reported role of NPC in aging. More interestingly, additional copies of plasmids expressing the mRNA export machinery Mex67 or Dbp5 (Figure 4C) significantly suppressed the growth reduction in *sus1Δ* cells, although there were no effects of the plasmids encoding *MTR2* or *NAB2*, which are genes encoding a cofactor of Mex67 and a physiological target of Dbp5, respectively [39, 40], on the growth of the *sus1Δ* strain. Furthermore, it was previously reported that *sus1Δ* is synthetically lethal with *dbp5* or *mex67* mutant alleles [20]. The *MEX67*-DAmP strain, in which mRNA destabilization of an essential gene is generated by disruption of its natural 3'-untranslated region [41], but not the *MTR2*-DAmP strain, showed a shortened lifespan (Figure 4D). Strikingly, consistent with the growth assay results in Figure 4B, the existence of library plasmids encoding *MEX67* or *DBP5* significantly restored the decreased lifespan of the *sus1Δ* strain (Figure 4E). Moreover, the strong overexpression of the single *MEX67* gene rescued cell proliferation and RLS impaired by *SUS1* loss (Figure 4F and 4G). In contrast to the growth and RLS results obtained from a library plasmid expressing *DBP5* (Figure 4B and 4E), Dbp5 expressed from pRS425 improved the shortened lifespan but not the impaired growth rate in *sus1Δ* cells (Figure 4F and 4G). Presumably, a proper dosage of *DBP5* is required to entirely overcome the cellular stress caused by Sus1 loss. Taken together, these results suggest that an increased dose of the mRNA export factors Mex67 and Dbp5 helps circumvent the growth and lifespan defects derived from Sus1 loss.

Increased *MEX67* or *DBP5* expression rescues the mRNA export defect in *sus1Δ* cells

Mutants of various factors involved in mRNA export, such as Sus1, induce nuclear retention of mRNA transcripts with poly(A)⁺ tails and sequester newly synthesized transcripts within nuclear foci at or near transcription sites [20, 42]. Given that multiple copies of the mRNA export factors Mex67 and Dbp5 compensate for the lifespan defect in *sus1Δ* cells, we next carried out poly(A)⁺ RNA fluorescence *in situ* hybridization (FISH) to determine whether Mex67 or Dbp5 would rescue the mRNA export defect of *sus1Δ* (Figure 5). Consistent with previous results in *sus1Δ* cells [20], we observed

nuclear accumulation of poly(A)⁺ RNA in cells lacking *SUS1* at 30°C, and the signal of the nuclear poly(A)⁺ signal became even stronger when cells were transferred to 37°C, likely reflecting the overproduction of heat shock mRNAs and an even more severe mRNA export defect (Supplementary Figure 4). In contrast to the impaired mRNA export in *sus1Δ* cells with an empty vector, mRNA export was fully rescued in WT *SUS1* gene-reintroduced *sus1Δ* cells (Figure 5A, lanes 1–3 and Supplementary Figure 5). Significantly, an extra copy of Mex67 or Dbp5 suppresses the accumulation of poly(A)⁺ RNA at nuclear foci in *sus1Δ* cells (Figure 5A, lanes 4 and 5 and Supplementary Figure 5), supporting the hypothesis that the enhanced mRNA export caused by an increased dosage of Mex67 or Dbp5 restores the mRNA export defect and impairs lifespan in cells lacking *SUS1*.

Sus1 is required for Dbp5 localization at the nuclear rim

Finally, we determined why the *sus1* deletion-mediated inhibition of mRNA nuclear export was reversed by the additional presence of general mRNA export factors. Mex67 and its heterodimeric partner Mtr2 are generally localized to the entire nuclear rim [43]. However, the subcellular location of Mex67 was altered and focused exclusively on some sites at the nuclear rim in *sac3* mutants [34, 44]. Additionally, Mex67 localization was partially affected by *Sus1* loss [34]. Therefore, to evaluate the effects of *Sus1* on the positioning of mRNA export factors at the nuclear rim, we monitored the nuclear location of green fluorescent protein (GFP)-tagged Dbp5 via fluorescence microscopy analysis (Figure 6). As expected, strong foci generated by

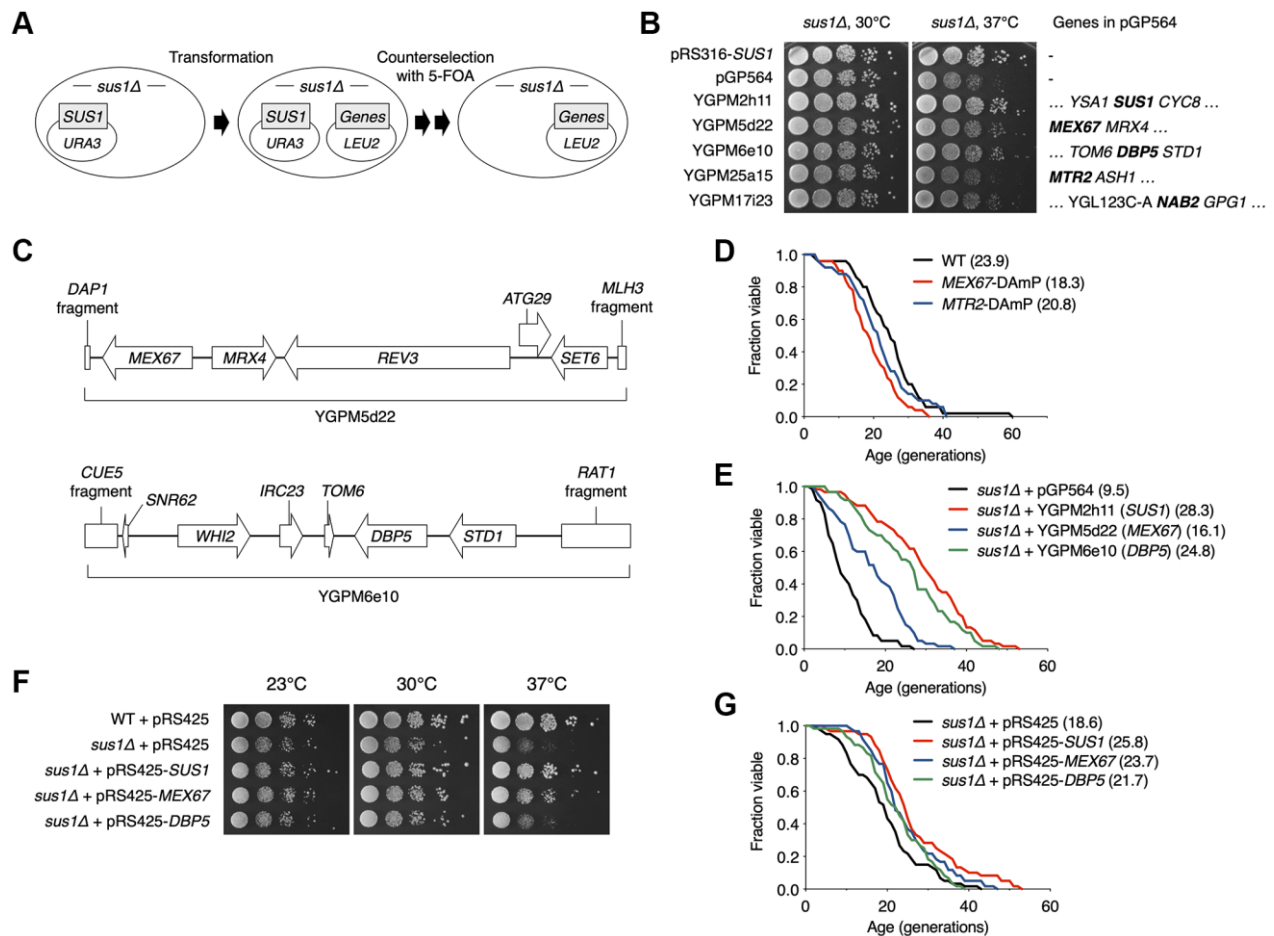


Figure 4. Multiple copies of *MEX67* or *DBP5* rescue impaired RLS in *sus1Δ* cells. (A) Strategy used to identify specific genes that suppress *sus1Δ* defects. *sus1Δ* cells containing pRS316-SUS1 were transformed with the indicated pGP564 (*LEU2*)-based plasmids, including NPC-related genes. Cells were streaked on SC-Trp-His-Leu supplemented with 5-FOA twice to evict pRS316-SUS1. (B) Growth analysis of WT or *sus1Δ* strains transformed with the indicated plasmids, as described in Figure 1E. Each gene on the plasmids is listed in the right panel. (C) Schematic diagrams of the YGPM5d22 (top) and YGPM6e10 (bottom) plasmids. The ORF locations (arrows or boxes) and gene names are indicated. (D and E) RLS analysis of the indicated mutants (D) and *sus1Δ* cells transformed with the indicated plasmids (E). The RLS analysis in (E) was carried out on SC-leu plate. The mean lifespans are shown in parentheses. (F) Growth analysis of WT or *sus1Δ* strains transformed with the indicated plasmids, as described in Figure 1E. (G) RLS analysis of *sus1Δ* cells transformed with the indicated plasmids was carried out on SC plate. The mean lifespans are shown in parentheses.

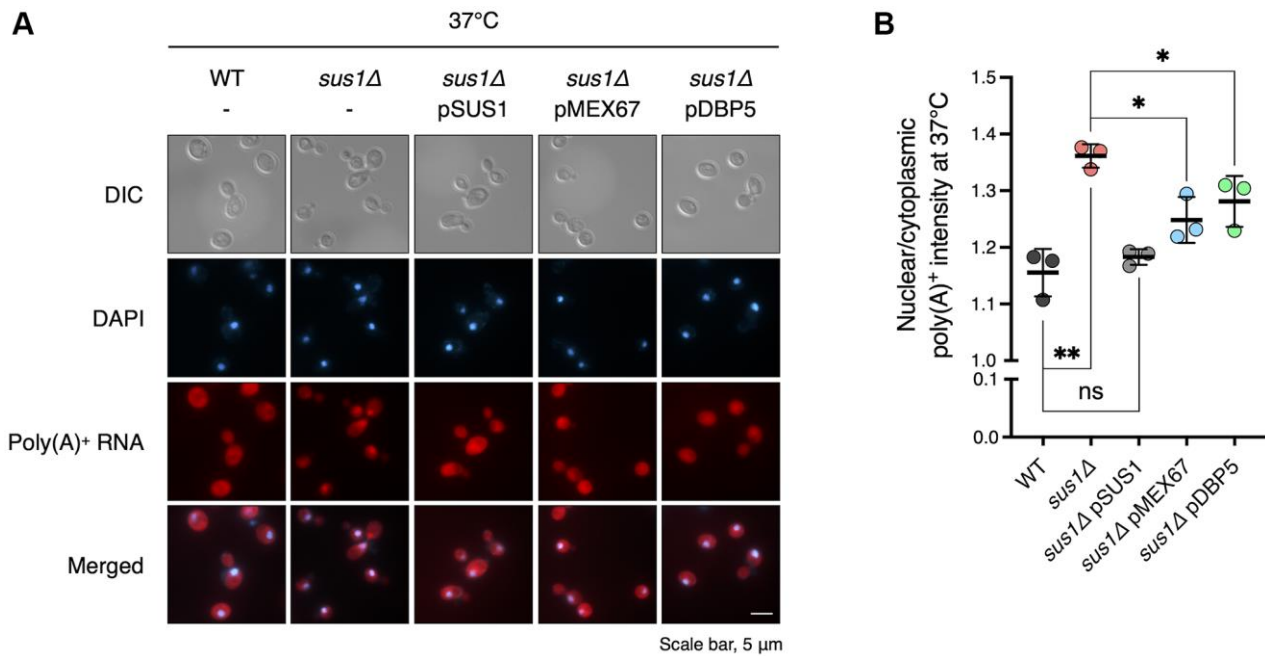


Figure 5. Increased doses of *MEX67* or *DBP5* restore the mRNA export defect in *sus1Δ* strains. (A) Representative images of FISH analysis for the WT and *sus1Δ* strains containing pRS316 expressing the indicated genes. Poly(A)⁺ RNAs were hybridized with Cy3-labeled oligo(dT) probes and visualized via fluorescence microscopy. DNA was stained with DAPI. DIC, DAPI, poly(A)⁺ RNA, and merged images are shown. (B) Quantitative analysis of the FISH results in (A). The nuclear poly(A)⁺ RNA intensity in each cell was divided by the cytoplasmic poly(A)⁺ RNA signal in the corresponding cell. Data are the mean ± SD of triplicate experiments. ***P* < 0.01; **P* < 0.05; ns, not significant (Student's *t*-test between the indicated pairs of values).

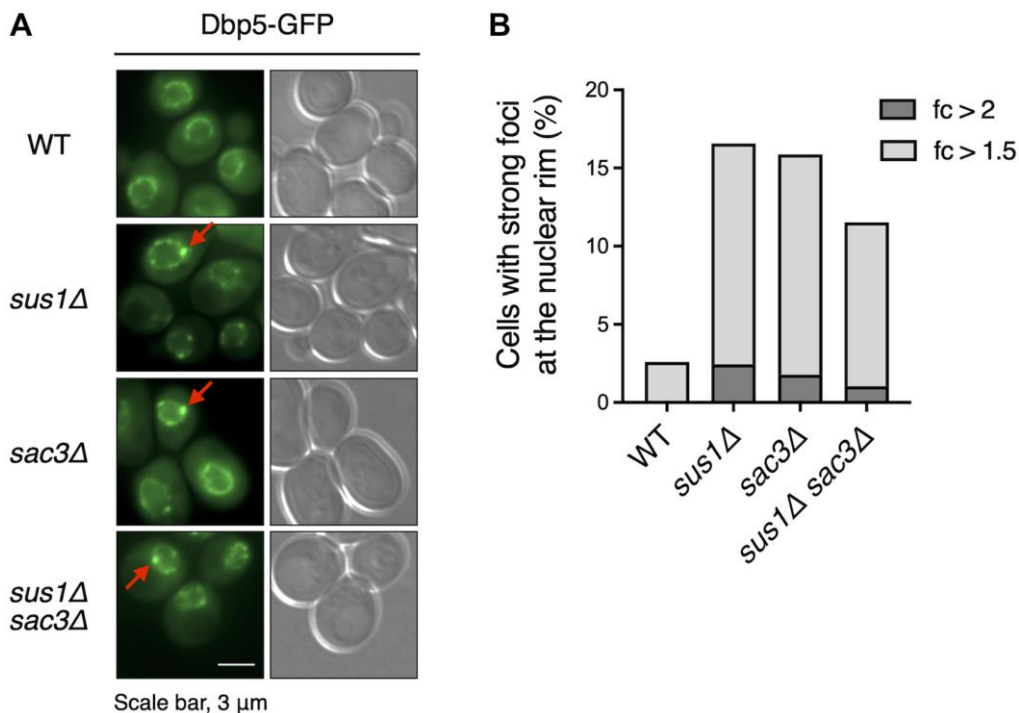


Figure 6. Dbp5 is mislocalized in *sus1Δ* cells. (A) Fluorescence microscopy analysis of Dbp5-GFP in WT cells and the indicated mutants. The left and right panels show GFP and DIC images, respectively. Red arrows indicate strong foci at the nuclear rim. (B) The percentage of cells containing strong Dbp5-GFP foci shown in (A). The ratio of the GFP intensity of each strong focus to that in the outer region of the strong focus was calculated. Light and dark gray color bars in the graph indicate the percentage of cells with >1.5- and 2-fold of the focus ratio, respectively.

Dbp5-GFP mislocalization at the nuclear rim increased greatly in *sac3Δ* cells. In particular, the ratio of the GFP intensity of the strong focus to the rest of the nuclear rim in *sus1Δ* cells was elevated to a level similar to that in *sac3Δ* cells. However, *sus1Δ sac3Δ* double mutants did not show any additional defect, suggesting that the two genes are epistatic and that mRNA export factor mislocalization in *sus1Δ* cells may be a critical reason for the accumulation of nuclear poly(A)⁺ RNA. Therefore, these results, together with the RLS (Figure 4) and poly(A)⁺ RNA FISH (Figure 5) data, strongly suggest that Sus1 is required for maintaining a normal lifespan through mRNA export control.

DISCUSSION

We revealed that Sus1, a co-subunit of SAGA and TREX-2, is a novel regulatory factor in lifespan regulation in yeast. Although many factors affect yeast lifespan in a Sir2-dependent manner, Sus1-mediated maintenance of the normal lifespan is dependent on NPC-associated TREX-2 but not on SAGA. An mRNA export defect caused by *SUS1* loss is restored by an increased dosage of the NPC anchoring-dependent mRNA export factors Mex67 and Dbp5, resulting in the rescue of RLS in *sus1Δ* cells. Furthermore, Sus1 is necessary for the cellular localization of Mex67 and Dbp5. Therefore, Sus1 integrates two processes, mRNA export and lifespan control, to maintain the youthful state of the nucleus by blocking the abnormal accumulation of mature mRNA in the nucleus.

SAGA plays multiple roles in transcription, including histone modification and RNA metabolism [14], and losses of its individual components differentially affect RLS in yeast [9, 11, 12], indicating that the complex network of subunits is needed to ensure a normal lifespan. Additionally, RLS is distinctly influenced by null mutants of nucleoporin proteins [32, 33]. The NPC is composed of diverse proteins that form the transport barrier [28], and its deterioration is considered as an aging marker [30, 31]. The cellular lifespan is a complex concept governed by multiple factors, and understanding such complex interactions is crucial for developing a new therapeutic strategy for age-related pathologies [45, 46].

Transcription accelerates the DNA damage rate, which can cause symptoms of genome instability and further premature aging [47]. The transcription error rate increases with aging and induces the aggregation of peptides associated with age-related disorders [48]. Additionally, diverse transcription factors can act as regulators of lifespan in eukaryotes, reflecting a link between gene expression and aging [49–57]. Notably, nuclear events after transcription are certainly related to

cellular aging. In *Drosophila*, sensitivity to environmental stress is increased and lifespan is reduced by mutation of the THO complex involved in transcription elongation and mRNA export [58]. The decreased turnover rate of human RNA caused by oxidative stress or reduced RNA exosome activity is one of the main causes of cellular senescence [59]. *PHO84* gene expression is repressed by its antisense RNA transcript in chronologically aged yeast cells, and antisense RNA stabilization is governed by the Rrp6 exosome and histone acetylation [60]. Therefore, to prevent pathophysiological cell senescence and cell death, it is important to identify mechanisms that inhibit transcription errors, nuclear accumulation of RNA, and abnormal export of mature RNA. The newly identified aging factor Sus1 is conserved in higher eukaryotes and appears to be important for maintaining the optimal balance of such mechanisms.

MATERIALS AND METHODS

Yeast strains

The yeast strains used in this study are listed in Supplementary Table 1. Standard techniques were used for strain construction. The deletion strains were generated by replacing each open reading frame (ORF) with *KanMX* modules constructed via polymerase chain reaction (PCR) amplification from the corresponding strains obtained from EUROSCARF or the pFA6a-KanMX6 or *HIS3MX6* module derived from pFA6a-HIS3MX6 [61]. The SY1031 strain was generated by switching *HIS3MX6*, used as a marker of DBP5-GFP in FY740, to *KIURA3* obtained from pFA6a-GFP-KIURA3 (Sung et al. 2008). To generate the SY1035 strain, the C-terminal insertion cassette of *SUS1-HA* was constructed by PCR amplification from pFA6a-HA-KIURA3 [62] and used to transform BY4741 cells. For the SY1036 and SY1037 strains, *MEX67-GFP* of FY739 and *DBP5-GFP* of FY740 were individually swapped by C-terminal HA tagging cassettes derived from pFA6a-HA-KIURA3 [62]. All strains were verified by PCR and/or immunoblot analysis.

Plasmids

The plasmids used in this study were created as described previously [63] and are listed in Supplementary Table 2. To make pRS316-SUS1, pRS316-MEX67, and pRS316-DBP5, the ORFs of *SUS1*, *MEX67*, and *DBP5*, including 900 bp upstream and 900 bp downstream, were individually PCR-amplified from yeast genomic DNA (BY4741) and cloned into pRS316. To create pRS425-SUS1, pRS425-MEX67, and pRS425-DBP5, *SUS1*, *MEX67*, and *DBP5* tagged with a sequence for the triplicate HA epitope,

including 900 bp upstream and 700 bp downstream of the ORF, were PCR-amplified from SY1035, SY1036, and SY1037, respectively, and cloned into pRS425. All constructs were confirmed by DNA sequencing.

Spotting assay

The spotting assay was performed as described previously [64]. Liquid cultures in exponential growth were normalized to 0.1 OD₆₀₀ and subjected to 10-fold serial dilutions. Cells were spotted onto YPD medium with or without 150 mM HU or SC medium with the appropriate amino acids and bases, and the plates were incubated at 16°C, 23°C, 30°C, or 37°C for 2–5 days. For *URA3*-based rDNA silencing analysis, strains containing the *URA3* gene at rDNA loci were used as described previously [65]. The pregrown cells were normalized to 1.0 OD₆₀₀ and then diluted with 5-fold serial dilutions. Cells were spotted onto SC medium with or without uracil or containing 5-FOA, and the plates were incubated at 30°C for 2–3 days.

RLS analysis

The RLS of yeast strains was measured on YPD plates, unless otherwise indicated, as described previously [12, 66]. A total of ~50 virgin daughter cells were subjected to lifespan analysis. To assess lifespan differences, a Mann–Whitney test was performed with a cutoff of $P = 0.05$. The average lifespan was considered different when $P < 0.05$ [4]. The comparison values between the control and each mutant are listed in Supplementary Table 3.

Fluorescence microscopy analysis

Images were acquired using an AxioCam HRm mounted on an Axio Observer Z1 microscope with a Plan-Apochromat 100 × /1.40 Oil DIC M27 objective lens, as reported previously [12]. Zeiss Filter Sets 38 HE (489038-9901-000), 20 (488020-9901-000), and 49 (488049-9901-000) were used to observe the fluorescence of GFP (excitation, 488 nm; emission, 509 nm), Cy3 (excitation, 549 nm; emission, 562 nm), and 4',6-diamidino-2-phenylindole (DAPI; excitation, 359 nm; emission, 463 nm), respectively. ZEN 2012 Blue Edition software was used to acquire and process each fluorescence image.

Dbp5-GFP foci formation was determined as described previously [34, 44]. The GFP fluorescence intensity was measured using ImageJ software. The GFP intensity of each strong focus was divided by that of the outer region of the strong focus in the corresponding cell, and the calculated ratio was collected from at least 1,000 cells per strain.

Poly(A)⁺ RNA FISH

Poly(A)⁺ RNA FISH was performed as described previously with minor modifications [67]. Yeast cells were grown in 10 ml SC-Ura medium at 30°C to 0.3 OD₆₀₀. Each culture was then divided into two halves and incubated for 2 h at 30°C or 37°C. Cells were crosslinked by adding a 1:10 volume of 37% (w/v) formaldehyde and incubated for 1 h at room temperature. Crosslinked cells were washed twice with 0.1 M potassium phosphate buffer (pH 6.5) and once with 1.2 M sorbitol/0.1 M potassium phosphate buffer (pH 6.5). The washed cells were allowed to adhere to a 0.3% poly-L-lysine (Sigma)-coated 10-well slide. The cell wall was digested by treatment with 250 µg/ml Zymolyase 20T (MP Bio) for 20 min. Cells were washed and hybridized with hybridization solution [50% deionized formamide, 4× SSC, 1× Denhardt's solution, 125 µg/ml tRNA (Sigma), 10% dextran sulfate, 500 µg/ml denatured salmon sperm DNA (Sigma), 50 pM Cy3-labeled oligo(dT)₃₀ (custom-synthesized by Integrated DNA Technologies)] overnight at 37°C in a humid chamber. After hybridization, the cells were washed, air-dried, and mounted with mounting solution [70% glycerol, 1× PBS, 1 mg/ml p-phenylenediamine, and 1 µg/ml DAPI (Sigma)]. ImageJ was used to detect nuclear and cytoplasmic Cy3 signals. At least 100 cells were examined for each of the three independent experiments. The significance of differences between the indicated strains was determined with a two-tailed, unpaired Student's *t*-test using GraphPad Prism software (** $P < 0.01$; * $P < 0.05$). Data represent the mean ± standard deviation (SD) of triplicate experiments.

Unequal sister chromatid exchange assay

The rate of marker loss through the unequal recombination of an *ADE2* marker inserted into the rDNA array was measured as reported previously [12, 65]. Cells grown to 1.0 OD₆₀₀ were plated at a density of ~400 cells per plate on SC plates containing a low adenine concentration (27 µM). The plates were incubated at 30°C for 2 or 3 days and then stored at 4°C for ~2 weeks to enhance the red color development. Colonies were counted using GeneTools software (Syngene). The percentage of marker loss was calculated by dividing the number of red-sectored colonies by the total number of colonies. Completely red colonies, indicating marker loss before plating, were excluded from the calculation.

AUTHOR CONTRIBUTIONS

S.H.A. organized and designed the scope of the study. H.-Y.R. wrote the manuscript with assistance from S.L., C.K. and S.H.A. S.L., Y.L. and B.-H.R. performed the

spotting assay and/or lifespan analysis. S.L. and Y.L. created the plasmids used in this study. S.L. performed spotting assays using a tiled yeast genomic DNA library, unequal sister chromatid exchange assays and all fluorescence microscopy analyses. S.L. and S.H.A. performed the data analysis for all experiments.

ACKNOWLEDGMENTS

We thank W.-K. Huh, S.-T. Kim, and M.S. Longtine for supplying the yeast strains and DNA constructs.

CONFLICTS OF INTEREST

The authors declare no conflicts of interest related to this study.

FUNDING

This study was supported by a National Research Foundation of Korea (NRF) grant funded by the South Korean government (MSIT) (no. 2021R1F1A1051082) to S.H.A. and (nos. 2020R1C1C1009367 and 2020R1A4A1018280) to H.-Y.R. and by the research fund of Hanyang University (HY-2022).

REFERENCES

1. Fontana L, Partridge L, Longo VD. Extending healthy life span--from yeast to humans. *Science*. 2010; 328:321–6.
<https://doi.org/10.1126/science.1172539>
PMID:20395504
2. Lai RW, Lu R, Danthi PS, Bravo JI, Goumba A, Sampathkumar NK, Benayoun BA. Multi-level remodeling of transcriptional landscapes in aging and longevity. *BMB Rep*. 2019; 52:86–108.
<https://doi.org/10.5483/BMBRep.2019.52.1.296>
PMID:30526773
3. Longo VD, Shadel GS, Kaeberlein M, Kennedy B. Replicative and chronological aging in *Saccharomyces cerevisiae*. *Cell Metab*. 2012; 16:18–31.
<https://doi.org/10.1016/j.cmet.2012.06.002>
PMID:22768836
4. Kaeberlein M, McVey M, Guarente L. The SIR2/3/4 complex and SIR2 alone promote longevity in *Saccharomyces cerevisiae* by two different mechanisms. *Genes Dev*. 1999; 13:2570–80.
<https://doi.org/10.1101/gad.13.19.2570>
PMID:10521401
5. Imai S, Armstrong CM, Kaeberlein M, Guarente L. Transcriptional silencing and longevity protein Sir2 is an NAD-dependent histone deacetylase. *Nature*. 2000; 403:795–800.
<https://doi.org/10.1038/35001622>
PMID:10693811
6. Dang W, Steffen KK, Perry R, Dorsey JA, Johnson FB, Shilatifard A, Kaeberlein M, Kennedy BK, Berger SL. Histone H4 lysine 16 acetylation regulates cellular lifespan. *Nature*. 2009; 459:802–7.
<https://doi.org/10.1038/nature08085>
PMID:19516333
7. Lee SH, Lee JH, Lee HY, Min KJ. Sirtuin signaling in cellular senescence and aging. *BMB Rep*. 2019; 52:24–34.
<https://doi.org/10.5483/BMBRep.2019.52.1.290>
PMID:30526767
8. Samara NL, Wolberger C. A new chapter in the transcription SAGA. *Curr Opin Struct Biol*. 2011; 21:767–74.
<https://doi.org/10.1016/j.sbi.2011.09.004>
PMID:22014650
9. Huang B, Zhong D, Zhu J, An Y, Gao M, Zhu S, Dang W, Wang X, Yang B, Xie Z. Inhibition of histone acetyltransferase GCN5 extends lifespan in both yeast and human cell lines. *Aging Cell*. 2020; 19:e13129.
<https://doi.org/10.1111/ace1.13129>
PMID:32157780
10. Horiuchi J, Silverman N, Marcus GA, Guarente L. ADA3, a putative transcriptional adaptor, consists of two separable domains and interacts with ADA2 and GCN5 in a trimeric complex. *Mol Cell Biol*. 1995; 15:1203–9.
<https://doi.org/10.1128/MCB.15.3.1203>
PMID:7862114
11. McCormick MA, Mason AG, Guyenet SJ, Dang W, Garza RM, Ting MK, Moller RM, Berger SL, Kaeberlein M, Pillus L, La Spada AR, Kennedy BK. The SAGA histone deubiquitinase module controls yeast replicative lifespan via Sir2 interaction. *Cell Rep*. 2014; 8:477–86.
<https://doi.org/10.1016/j.celrep.2014.06.037>
PMID:25043177
12. Lim S, Ahn H, Duan R, Liu Y, Ryu HY, Ahn SH. The Spt7 subunit of the SAGA complex is required for the regulation of lifespan in both dividing and nondividing yeast cells. *Mech Ageing Dev*. 2021; 196:111480.
<https://doi.org/10.1016/j.mad.2021.111480>
PMID:33831401
13. Denoth-Lippuner A, Krzyzanowski MK, Stober C, Barral Y. Role of SAGA in the asymmetric segregation of DNA circles during yeast ageing. *Elife*. 2014; 3:e03790.
<https://doi.org/10.7554/eLife.03790>
PMID:25402830

14. Rodríguez-Navarro S. Insights into SAGA function during gene expression. *EMBO Rep.* 2009; 10:843–50. <https://doi.org/10.1038/embor.2009.168> PMID:19609321
15. Fischer T, Strässer K, Rácz A, Rodríguez-Navarro S, Oppizzi M, Ihrig P, Lechner J, Hurt E. The mRNA export machinery requires the novel Sac3p-Thp1p complex to dock at the nucleoplasmic entrance of the nuclear pores. *EMBO J.* 2002; 21:5843–52. <https://doi.org/10.1093/emboj/cdf590> PMID:12411502
16. Lei EP, Stern CA, Fahrenkrog B, Krebber H, Moy TI, Aebi U, Silver PA. Sac3 is an mRNA export factor that localizes to cytoplasmic fibrils of nuclear pore complex. *Mol Biol Cell.* 2003; 14:836–47. <https://doi.org/10.1091/mbc.e02-08-0520> PMID:12631707
17. Jani D, Lutz S, Marshall NJ, Fischer T, Köhler A, Ellisdon AM, Hurt E, Stewart M. Sus1, Cdc31, and the Sac3 CID region form a conserved interaction platform that promotes nuclear pore association and mRNA export. *Mol Cell.* 2009; 33:727–37. <https://doi.org/10.1016/j.molcel.2009.01.033> PMID:19328066
18. Ellisdon AM, Dimitrova L, Hurt E, Stewart M. Structural basis for the assembly and nucleic acid binding of the TREX-2 transcription-export complex. *Nat Struct Mol Biol.* 2012; 19:328–36. <https://doi.org/10.1038/nsmb.2235> PMID:22343721
19. Jani D, Valkov E, Stewart M. Structural basis for binding the TREX2 complex to nuclear pores, GAL1 localisation and mRNA export. *Nucleic Acids Res.* 2014; 42:6686–97. <https://doi.org/10.1093/nar/gku252> PMID:24705649
20. Rodríguez-Navarro S, Fischer T, Luo MJ, Antúnez O, Brettschneider S, Lechner J, Pérez-Ortín JE, Reed R, Hurt E. Sus1, a functional component of the SAGA histone acetylase complex and the nuclear pore-associated mRNA export machinery. *Cell.* 2004; 116:75–86. [https://doi.org/10.1016/s0092-8674\(03\)01025-0](https://doi.org/10.1016/s0092-8674(03)01025-0) PMID:14718168
21. Köhler A, Pascual-García P, Llopis A, Zapater M, Posas F, Hurt E, Rodríguez-Navarro S. The mRNA export factor Sus1 is involved in Spt/Ada/Gcn5 acetyltransferase-mediated H2B deubiquitinylation through its interaction with Ubp8 and Sgf11. *Mol Biol Cell.* 2006; 17:4228–36. <https://doi.org/10.1091/mbc.e06-02-0098> PMID:16855026
22. Schneider M, Hellerschmied D, Schubert T, Amlacher S, Vinayachandran V, Reja R, Pugh BF, Clausen T, Köhler A. The Nuclear Pore-Associated TREX-2 Complex Employs Mediator to Regulate Gene Expression. *Cell.* 2015; 162:1016–28. <https://doi.org/10.1016/j.cell.2015.07.059> PMID:26317468
23. García-Molinero V, García-Martínez J, Reja R, Furió-Tarí P, Antúnez O, Vinayachandran V, Conesa A, Pugh BF, Pérez-Ortín JE, Rodríguez-Navarro S. The SAGA/TREX-2 subunit Sus1 binds widely to transcribed genes and affects mRNA turnover globally. *Epigenetics Chromatin.* 2018; 11:13. <https://doi.org/10.1186/s13072-018-0184-2> PMID:29598828
24. Cabal GG, Genovesio A, Rodríguez-Navarro S, Zimmer C, Gadal O, Lesne A, Buc H, Feuerbach-Fournier F, Olivo-Marin JC, Hurt EC, Nehrbass U. SAGA interacting factors confine sub-diffusion of transcribed genes to the nuclear envelope. *Nature.* 2006; 441:770–3. <https://doi.org/10.1038/nature04752> PMID:16760982
25. Kurshakova MM, Krasnov AN, Kopytova DV, Shidlovskii YV, Nikolenko JV, Nabirochkina EN, Spohner D, Schultz P, Tora L, Georgieva SG. SAGA and a novel Drosophila export complex anchor efficient transcription and mRNA export to NPC. *EMBO J.* 2007; 26:4956–65. <https://doi.org/10.1038/sj.emboj.7601901> PMID:18034162
26. Chekanova JA, Abruzzi KC, Rosbash M, Belostotsky DA. Sus1, Sac3, and Thp1 mediate post-transcriptional tethering of active genes to the nuclear rim as well as to non-nascent mRNP. *RNA.* 2008; 14:66–77. <https://doi.org/10.1261/rna.764108> PMID:18003937
27. Faza MB, Kemmler S, Jimeno S, González-Aguilera C, Aguilera A, Hurt E, Panse VG. Sem1 is a functional component of the nuclear pore complex-associated messenger RNA export machinery. *J Cell Biol.* 2009; 184:833–46. <https://doi.org/10.1083/jcb.200810059> PMID:19289793
28. Wente SR, Rout MP. The nuclear pore complex and nuclear transport. *Cold Spring Harb Perspect Biol.* 2010; 2:a000562. <https://doi.org/10.1101/cshperspect.a000562> PMID:20630994
29. Terry LJ, Wente SR. Flexible gates: dynamic topologies and functions for FG nucleoporins in nucleocytoplasmic transport. *Eukaryot Cell.* 2009; 8:1814–27.

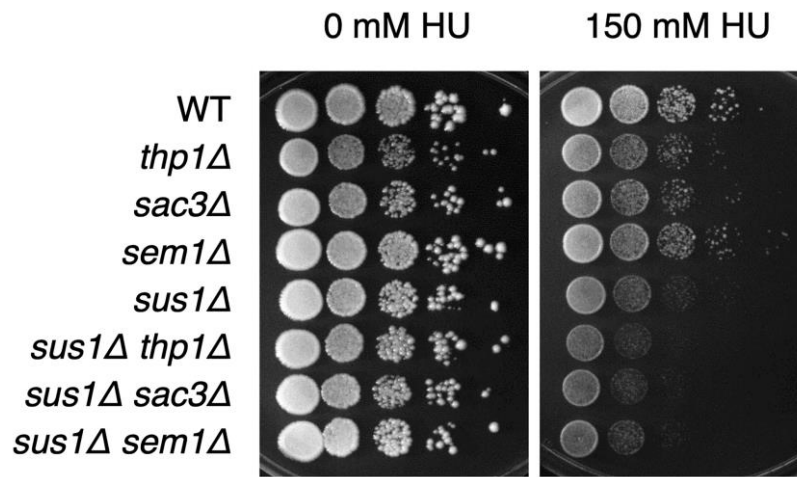
- <https://doi.org/10.1128/EC.00225-09>
PMID:[19801417](https://pubmed.ncbi.nlm.nih.gov/19801417/)
30. D'Angelo MA, Raices M, Panowski SH, Hetzer MW. Age-dependent deterioration of nuclear pore complexes causes a loss of nuclear integrity in postmitotic cells. *Cell*. 2009; 136:284–95.
<https://doi.org/10.1016/j.cell.2008.11.037>
PMID:[19167330](https://pubmed.ncbi.nlm.nih.gov/19167330/)
31. Savas JN, Toyama BH, Xu T, Yates JR 3rd, Hetzer MW. Extremely long-lived nuclear pore proteins in the rat brain. *Science*. 2012; 335:942.
<https://doi.org/10.1126/science.1217421>
PMID:[22300851](https://pubmed.ncbi.nlm.nih.gov/22300851/)
32. Lord CL, Timney BL, Rout MP, Wentz SR. Altering nuclear pore complex function impacts longevity and mitochondrial function in *S. cerevisiae*. *J Cell Biol*. 2015; 208:729–44.
<https://doi.org/10.1083/jcb.201412024>
PMID:[25778920](https://pubmed.ncbi.nlm.nih.gov/25778920/)
33. Lord CL, Ospovat O, Wentz SR. Nup100 regulates *Saccharomyces cerevisiae* replicative life span by mediating the nuclear export of specific tRNAs. *RNA*. 2017; 23:365–77.
<https://doi.org/10.1261/rna.057612.116>
PMID:[27932586](https://pubmed.ncbi.nlm.nih.gov/27932586/)
34. Pascual-García P, Govind CK, Queralt E, Cuenca-Bono B, Llopis A, Chavez S, Hinnebusch AG, Rodríguez-Navarro S. Sus1 is recruited to coding regions and functions during transcription elongation in association with SAGA and TREX2. *Genes Dev*. 2008; 22:2811–22.
<https://doi.org/10.1101/gad.483308>
PMID:[18923079](https://pubmed.ncbi.nlm.nih.gov/18923079/)
35. González-Aguilera C, Tous C, Gómez-González B, Huertas P, Luna R, Aguilera A. The THP1-SAC3-SUS1-CDC31 complex works in transcription elongation-mRNA export preventing RNA-mediated genome instability. *Mol Biol Cell*. 2008; 19:4310–8.
<https://doi.org/10.1091/mbc.e08-04-0355>
PMID:[18667528](https://pubmed.ncbi.nlm.nih.gov/18667528/)
36. Sinclair DA, Guarente L. Extrachromosomal rDNA circles—a cause of aging in yeast. *Cell*. 1997; 91:1033–42.
[https://doi.org/10.1016/s0092-8674\(00\)80493-6](https://doi.org/10.1016/s0092-8674(00)80493-6)
PMID:[9428525](https://pubmed.ncbi.nlm.nih.gov/9428525/)
37. García-Oliver E, García-Molinero V, Rodríguez-Navarro S. mRNA export and gene expression: the SAGA-TREX-2 connection. *Biochim Biophys Acta*. 2012; 1819:555–65.
<https://doi.org/10.1016/j.bbagr.2011.11.011>
PMID:[22178374](https://pubmed.ncbi.nlm.nih.gov/22178374/)
38. Rout MP, Aitchison JD, Suprpto A, Hjertaas K, Zhao Y, Chait BT. The yeast nuclear pore complex: composition, architecture, and transport mechanism. *J Cell Biol*. 2000; 148:635–51.
<https://doi.org/10.1083/jcb.148.4.635>
PMID:[10684247](https://pubmed.ncbi.nlm.nih.gov/10684247/)
39. Tran EJ, Zhou Y, Corbett AH, Wentz SR. The DEAD-box protein Dbp5 controls mRNA export by triggering specific RNA:protein remodeling events. *Mol Cell*. 2007; 28:850–9.
<https://doi.org/10.1016/j.molcel.2007.09.019>
PMID:[18082609](https://pubmed.ncbi.nlm.nih.gov/18082609/)
40. Yao W, Roser D, Köhler A, Bradatsch B, Bassler J, Hurt E. Nuclear export of ribosomal 60S subunits by the general mRNA export receptor Mex67-Mtr2. *Mol Cell*. 2007; 26:51–62.
<https://doi.org/10.1016/j.molcel.2007.02.018>
PMID:[17434126](https://pubmed.ncbi.nlm.nih.gov/17434126/)
41. Breslow DK, Cameron DM, Collins SR, Schuldiner M, Stewart-Ornstein J, Newman HW, Braun S, Madhani HD, Krogan NJ, Weissman JS. A comprehensive strategy enabling high-resolution functional analysis of the yeast genome. *Nat Methods*. 2008; 5:711–8.
<https://doi.org/10.1038/nmeth.1234>
PMID:[18622397](https://pubmed.ncbi.nlm.nih.gov/18622397/)
42. Jensen TH, Patricio K, McCarthy T, Rosbash M. A block to mRNA nuclear export in *S. cerevisiae* leads to hyperadenylation of transcripts that accumulate at the site of transcription. *Mol Cell*. 2001; 7:887–98.
[https://doi.org/10.1016/s1097-2765\(01\)00232-5](https://doi.org/10.1016/s1097-2765(01)00232-5)
PMID:[11336711](https://pubmed.ncbi.nlm.nih.gov/11336711/)
43. Lim S, Kwak J, Kim M, Lee D. Separation of a functional deubiquitylating module from the SAGA complex by the proteasome regulatory particle. *Nat Commun*. 2013; 4:2641.
<https://doi.org/10.1038/ncomms3641>
PMID:[24136112](https://pubmed.ncbi.nlm.nih.gov/24136112/)
44. Köhler A, Schneider M, Cabal GG, Nehrbass U, Hurt E. Yeast Ataxin-7 links histone deubiquitination with gene gating and mRNA export. *Nat Cell Biol*. 2008; 10:707–15.
<https://doi.org/10.1038/ncb1733>
PMID:[18488019](https://pubmed.ncbi.nlm.nih.gov/18488019/)
45. Dolivo D, Hernandez S, Dominko T. Cellular lifespan and senescence: a complex balance between multiple cellular pathways. *Bioessays*. 2016 (Suppl 1); 38:S33–44.
<https://doi.org/10.1002/bies.201670906>
PMID:[27417120](https://pubmed.ncbi.nlm.nih.gov/27417120/)
46. Lee JS. Cellular senescence, aging, and age-related disease: Special issue of BMB Reports in 2019. *BMB Rep*. 2019; 52:1–2.
<https://doi.org/10.5483/BMBRep.2019.52.1.002>
PMID:[30638180](https://pubmed.ncbi.nlm.nih.gov/30638180/)

47. Callegari AJ. Does transcription-associated DNA damage limit lifespan? *DNA Repair (Amst)*. 2016; 41:1–7.
<https://doi.org/10.1016/j.dnarep.2016.03.001>
PMID:[27010736](https://pubmed.ncbi.nlm.nih.gov/27010736/)
48. Vermulst M, Denney AS, Lang MJ, Hung CW, Moore S, Moseley MA, Thompson JW, Madden V, Gauer J, Wolfe KJ, Summers DW, Schleit J, Sutphin GL, et al. Transcription errors induce proteotoxic stress and shorten cellular lifespan. *Nat Commun*. 2015; 6: 8065.
<https://doi.org/10.1038/ncomms9065>
PMID:[26304740](https://pubmed.ncbi.nlm.nih.gov/26304740/)
49. Oh SW, Mukhopadhyay A, Svrzikapa N, Jiang F, Davis RJ, Tissenbaum HA. JNK regulates lifespan in *Caenorhabditis elegans* by modulating nuclear translocation of forkhead transcription factor/DAF-16. *Proc Natl Acad Sci U S A*. 2005; 102:4494–9.
<https://doi.org/10.1073/pnas.0500749102>
PMID:[15767565](https://pubmed.ncbi.nlm.nih.gov/15767565/)
50. Ghazi A, Henis-Korenblit S, Kenyon C. A transcription elongation factor that links signals from the reproductive system to lifespan extension in *Caenorhabditis elegans*. *PLoS Genet*. 2009; 5:e1000639.
<https://doi.org/10.1371/journal.pgen.1000639>
PMID:[19749979](https://pubmed.ncbi.nlm.nih.gov/19749979/)
51. Yamamoto R, Tatar M. Insulin receptor substrate chico acts with the transcription factor FOXO to extend *Drosophila* lifespan. *Aging Cell*. 2011; 10:729–32.
<https://doi.org/10.1111/j.1474-9726.2011.00716.x>
PMID:[21518241](https://pubmed.ncbi.nlm.nih.gov/21518241/)
52. Postnikoff SD, Malo ME, Wong B, Harkness TA. The yeast forkhead transcription factors fkh1 and fkh2 regulate lifespan and stress response together with the anaphase-promoting complex. *PLoS Genet*. 2012; 8:e1002583.
<https://doi.org/10.1371/journal.pgen.1002583>
PMID:[22438832](https://pubmed.ncbi.nlm.nih.gov/22438832/)
53. Cai L, McCormick MA, Kennedy BK, Tu BP. Integration of multiple nutrient cues and regulation of lifespan by ribosomal transcription factor Ifh1. *Cell Rep*. 2013; 4:1063–71.
<https://doi.org/10.1016/j.celrep.2013.08.016>
PMID:[24035395](https://pubmed.ncbi.nlm.nih.gov/24035395/)
54. Alic N, Giannakou ME, Papatheodorou I, Hoddinott MP, Andrews TD, Bolukbasi E, Partridge L. Interplay of dFOXO and two ETS-family transcription factors determines lifespan in *Drosophila melanogaster*. *PLoS Genet*. 2014; 10:e1004619.
<https://doi.org/10.1371/journal.pgen.1004619>
PMID:[25232726](https://pubmed.ncbi.nlm.nih.gov/25232726/)
55. Ryu HY, Rhie BH, Ahn SH. Loss of the Set2 histone methyltransferase increases cellular lifespan in yeast cells. *Biochem Biophys Res Commun*. 2014; 446:113–8.
<https://doi.org/10.1016/j.bbrc.2014.02.061>
PMID:[24607280](https://pubmed.ncbi.nlm.nih.gov/24607280/)
56. Mittal N, Guimaraes JC, Gross T, Schmidt A, Vina-Vilaseca A, Nedialkova DD, Aeschmann F, Leidel SA, Spang A, Zavolan M. The Gcn4 transcription factor reduces protein synthesis capacity and extends yeast lifespan. *Nat Commun*. 2017; 8:457.
<https://doi.org/10.1038/s41467-017-00539-y>
PMID:[28878244](https://pubmed.ncbi.nlm.nih.gov/28878244/)
57. Rodríguez-López M, Gonzalez S, Hillson O, Tunnaciff E, Codlin S, Tallada VA, Bähler J, Rallis C. The GATA Transcription Factor Gaf1 Represses tRNAs, Inhibits Growth, and Extends Chronological Lifespan Downstream of Fission Yeast TORC1. *Cell Rep*. 2020; 30:3240–9.e4.
<https://doi.org/10.1016/j.celrep.2020.02.058>
PMID:[32160533](https://pubmed.ncbi.nlm.nih.gov/32160533/)
58. Moon S, Cho B, Min SH, Lee D, Chung YD. The THO complex is required for nucleolar integrity in *Drosophila* spermatocytes. *Development*. 2011; 138:3835–45.
<https://doi.org/10.1242/dev.056945>
PMID:[21828100](https://pubmed.ncbi.nlm.nih.gov/21828100/)
59. Mullani N, Porozhan Y, Mangelinck A, Rachez C, Costallat M, Batsché E, Goodhardt M, Cenci G, Mann C, Muchardt C. Reduced RNA turnover as a driver of cellular senescence. *Life Sci Alliance*. 2021; 4:e202000809.
<https://doi.org/10.26508/lsa.202000809>
PMID:[33446491](https://pubmed.ncbi.nlm.nih.gov/33446491/)
60. Camblong J, Iglesias N, Fickentscher C, Dieppo G, Stutz F. Antisense RNA stabilization induces transcriptional gene silencing via histone deacetylation in *S. cerevisiae*. *Cell*. 2007; 131:706–17.
<https://doi.org/10.1016/j.cell.2007.09.014>
PMID:[18022365](https://pubmed.ncbi.nlm.nih.gov/18022365/)
61. Longtine MS, McKenzie A 3rd, Demarini DJ, Shah NG, Wach A, Brachat A, Philippsen P, Pringle JR. Additional modules for versatile and economical PCR-based gene deletion and modification in *Saccharomyces cerevisiae*. *Yeast*. 1998; 14:953–61.
[https://doi.org/10.1002/\(SICI\)1097-0061\(199807\)14:10<953::AID-YEA293>3.0.CO;2-U](https://doi.org/10.1002/(SICI)1097-0061(199807)14:10<953::AID-YEA293>3.0.CO;2-U)
PMID:[9717241](https://pubmed.ncbi.nlm.nih.gov/9717241/)
62. Sung MK, Ha CW, Huh WK. A vector system for efficient and economical switching of C-terminal epitope tags in *Saccharomyces cerevisiae*. *Yeast*. 2008; 25:301–11.
<https://doi.org/10.1002/yea.1588>
PMID:[18350525](https://pubmed.ncbi.nlm.nih.gov/18350525/)

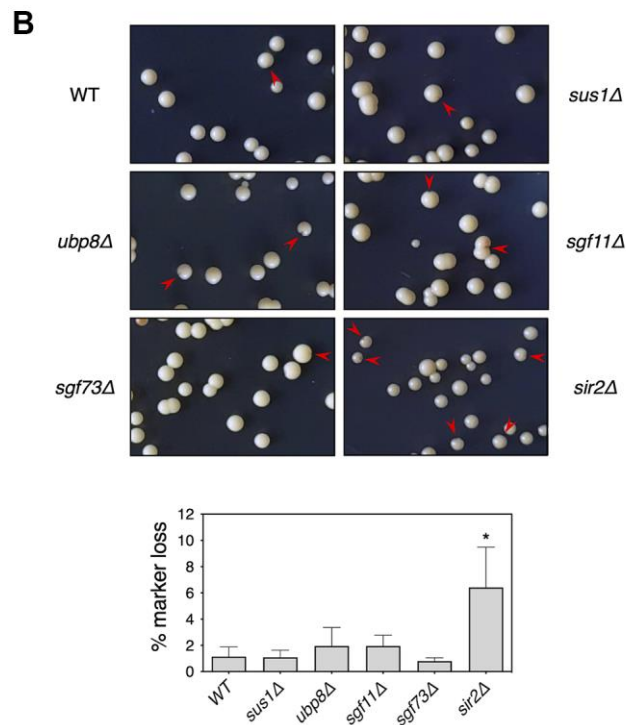
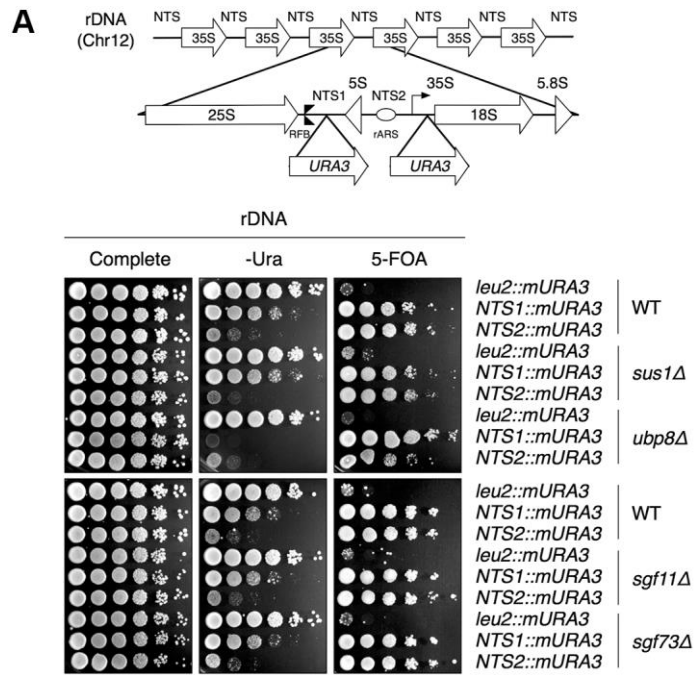
63. Ryu HY, López-Giráldez F, Knight J, Hwang SS, Renner C, Kreft SG, Hochstrasser M. Distinct adaptive mechanisms drive recovery from aneuploidy caused by loss of the Ulp2 SUMO protease. *Nat Commun.* 2018; 9:5417.
<https://doi.org/10.1038/s41467-018-07836-0>
PMID:[30575729](https://pubmed.ncbi.nlm.nih.gov/30575729/)
64. Ryu HY, Wilson NR, Mehta S, Hwang SS, Hochstrasser M. Loss of the SUMO protease Ulp2 triggers a specific multichromosome aneuploidy. *Genes Dev.* 2016; 30:1881–94.
<https://doi.org/10.1101/gad.282194.116>
PMID:[27585592](https://pubmed.ncbi.nlm.nih.gov/27585592/)
65. Ryu HY, Ahn S. Yeast histone H3 lysine 4 demethylase Jhd2 regulates mitotic rDNA condensation. *BMC Biol.* 2014; 12:75.
<https://doi.org/10.1186/s12915-014-0075-3>
PMID:[25248920](https://pubmed.ncbi.nlm.nih.gov/25248920/)
66. Rhie BH, Song YH, Ryu HY, Ahn SH. Cellular aging is associated with increased ubiquitylation of histone H2B in yeast telomeric heterochromatin. *Biochem Biophys Res Commun.* 2013; 439:570–5.
<https://doi.org/10.1016/j.bbrc.2013.09.017>
PMID:[24025678](https://pubmed.ncbi.nlm.nih.gov/24025678/)
67. Cuenca-Bono B, García-Molinero V, Pascual-García P, Dopazo H, Llopis A, Vilardell J, Rodríguez-Navarro S. SUS1 introns are required for efficient mRNA nuclear export in yeast. *Nucleic Acids Res.* 2011; 39:8599–611.
<https://doi.org/10.1093/nar/gkr496>
PMID:[21749979](https://pubmed.ncbi.nlm.nih.gov/21749979/)

SUPPLEMENTARY MATERIALS

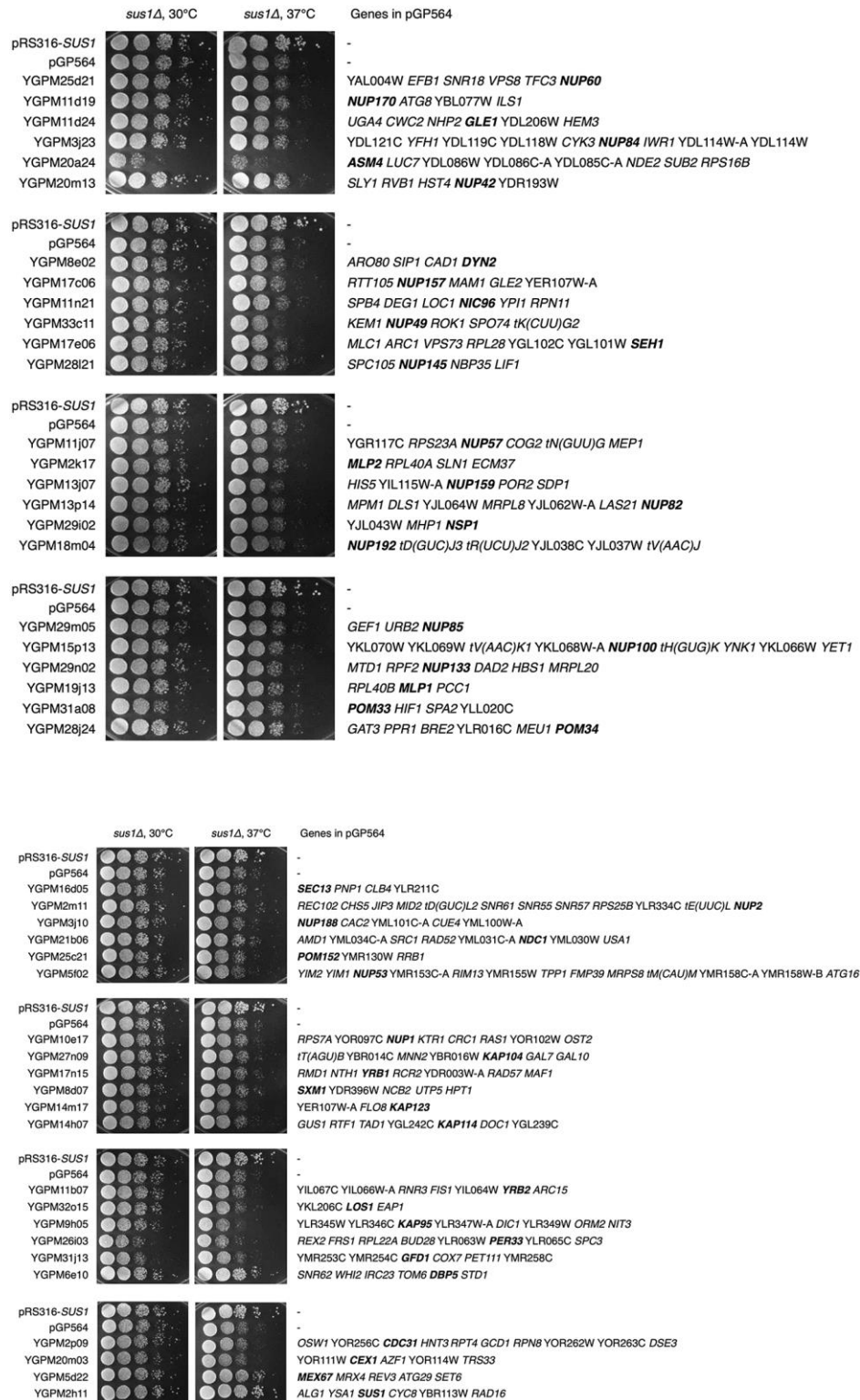
Supplementary Figures



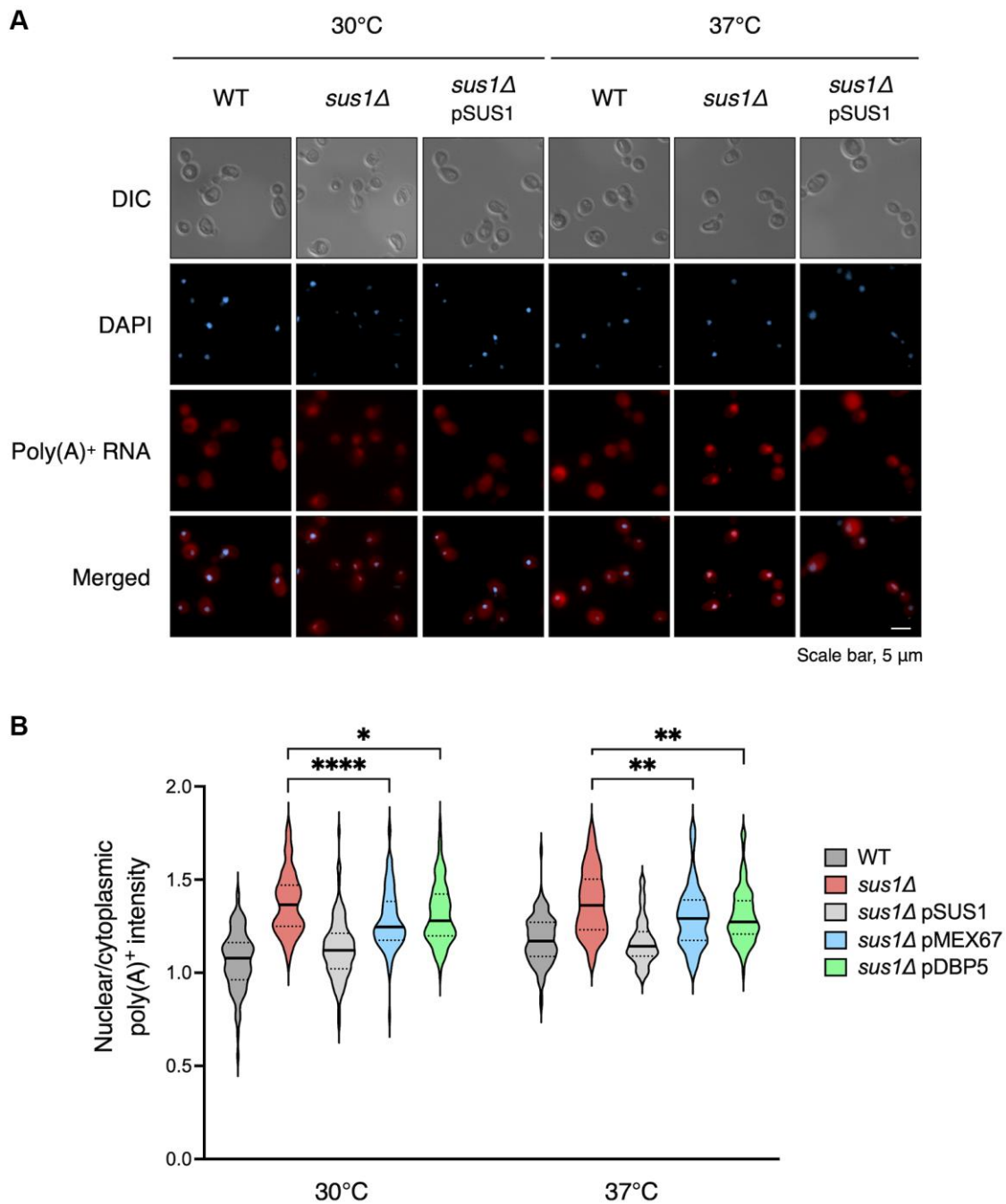
Supplementary Figure 1. HU sensitivity assays in double deletion *sus1Δ* strains with TREX-2 mutants. The indicated mutants were spotted onto YPD plates with or without 150 mM HU, as described in Figure 1E.



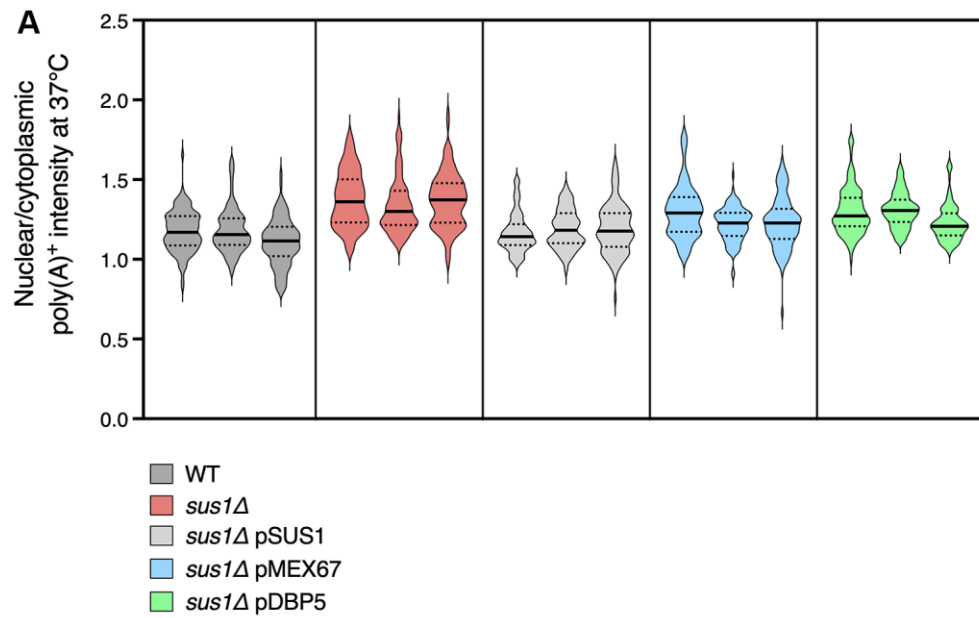
Supplementary Figure 2. *SUS1* deletion does not affect rDNA silencing and recombination. (A) Schematic diagram (top) showing an rDNA unit embedded within a tandem array on chromosome XII with the position of *mURA3* reporters inserted into NTS1 or NTS2. The 35S pre-rRNA encoding the 18S, 5.8S, and 25S rRNAs is separated by NTS1 and NTS2. The locations of RFB (double triangle), ARS replication origin (oval), 5S rRNA gene (triangle), and 35S transcription start site (bent arrow) are represented. *URA3*-based rDNA silencing assays (bottom) were carried out in DMY2798 (*leu2::mURA3*), DMY2804 (*RDN1-NTS1::mURA3*), or DMY2800 (*RDN1-NTS2::mURA3*) strains with the indicated deletions. (B) The frequency of unequal rDNA crossovers was monitored by loss of the *ADE2* gene located within the rDNA array for the WT (W303R) strain and the indicated deletion strains. Pictures of plates are shown in the top panels. The percentage of *ADE2* gene loss (% marker loss) was calculated as the ratio of red-colored colonies to the total number of colonies and is shown in the bottom panel. Completely red colonies were excluded. Error bars indicate the SD from two repetitions, and asterisks indicate statistically significant differences between the mutant and WT strains (ns, not significant; * $P < 0.05$).



Supplementary Figure 3. Screening of NPC-related genes for the suppression of growth defects in *sus1Δ* cells. Growth analysis of *sus1Δ* strains, including the indicated plasmids, as described in Figure 1E. Genes on the plasmids (pGP564) are listed on the right of each panel.



Supplementary Figure 4. The mRNA export defect induced by *sus1Δ* was observed at both 30°C and 37°C. (A) Poly(A)⁺ RNA FISH analysis of the WT, *sus1Δ*, and *sus1Δ* containing pRS316-SUS1 strains, as described in Figure 5A. **(B)** Violin plot of poly(A)⁺ RNA FISH results for the strains used in Figure 5A at both 30°C and 37°C. The medians and quartiles are marked as thick and dotted lines, respectively. **** $P < 0.0001$; ** $P < 0.01$; * $P < 0.05$ (Student's *t*-test between the indicated pairs of values).



B

Experiments	Cell numbers	Mean (Nuclear/cytoplasmic poly(A) ⁺ intensity at 37°C)
1		
WT	103	1.176154
<i>sus1Δ</i>	112	1.376510
<i>sus1Δ</i> pSUS1	100	1.167284
<i>sus1Δ</i> pMEX67	104	1.294548
<i>sus1Δ</i> pDBP5	103	1.304344
2		
WT	102	1.182704
<i>sus1Δ</i>	105	1.337783
<i>sus1Δ</i> pSUS1	105	1.188931
<i>sus1Δ</i> pMEX67	103	1.218946
<i>sus1Δ</i> pDBP5	104	1.309805
3		
WT	103	1.107127
<i>sus1Δ</i>	102	1.369916
<i>sus1Δ</i> pSUS1	102	1.192707
<i>sus1Δ</i> pMEX67	110	1.231505
<i>sus1Δ</i> pDBP5	104	1.229178

Supplementary Figure 5. Additional copies of *MEX67* or *DBP5* rescued the mRNA export defect in *sus1Δ* cells. (A) Violin plot of poly(A)⁺ RNA FISH results presented in Figure 5A, as described in Supplementary Figure 4B. The nuclear/cytoplasmic poly(A)⁺ intensity of each replicate is plotted. (B) The cell numbers and mean nuclear/cytoplasmic poly(A)⁺ intensity ratio in (A) are shown.

Supplementary Tables

Please browse Full Text version to see the data of Supplementary Table 1.

Supplementary Table 1. Strains used in this study.

Supplementary Table 2. Plasmids used in this study.

Name	Description	Source
pFA6a-HIS3MX6	<i>pBR322 origin, Amp^R, HIS3MX6, HIS3 gene from S. kluyveri.</i>	[2]
pFA6a-KanMX6	<i>pBR322 origin, Amp^R, KanMX6, KanMX gene contains the known kan^r ORF of the E. coli transposon Tn903.</i>	[2]
pFA6a-GFP-KIURA3	<i>pBR322 origin, Amp^R, URA3, GFP tag with URA3 gene</i>	[3]
pFA6a-HA-KIURA3	<i>pBR322 origin, Amp^R, URA3, Triple HA tag with URA3 gene</i>	[3]
pGP564	<i>2μ, Kan^R, LEU2</i>	[4]
YGPM2h11	<i>2μ, Kan^R, LEU2, [YBR109W-A]&, [ALG1], YSA1, SUS1, CYC8, YBR113W, RAD16, [LYS2]&</i>	[4]
YGPM5d22	<i>2μ, Kan^R, LEU2, [DAP1]&, MEX67, YPL168W, REV3, YPL166W, [SET6], [MLH3]&</i>	[4]
YGPM6e10	<i>2μ, Kan^R, LEU2, [CUE5]&, snR62, WHI2, YOR044W TOM6, DBP5, STD1, [RAT1]&</i>	[4]
YGPM25a15	<i>2μ, Kan^R, LEU2, [YKL187C]* MTR2 ASH1 SPE1 YKL183C-A [LOT5]*</i>	[4]
YGPM17i23	<i>2μ, Kan^R, LEU2, [RSM23]* CWC23 SOH1 SCS3 MET13 MON1 RPS2 YGL123C-A NAB2 GPG1 [PRP43]</i>	[4]
pRS316	<i>CEN/ARS, Amp^R, URA3</i>	[5]
pRS316-SUS1	<i>CEN/ARS, Amp^R, URA3, SUS1 ORF with +- 900 bp of UTR</i>	This study
pRS316-MEX67	<i>CEN/ARS, Amp^R, URA3, MEX67 ORF with +- 900 bp of UTR</i>	This study
pRS316-DBP5	<i>CEN/ARS, Amp^R, URA3, DBP5 ORF with +- 900 bp of UTR</i>	This study
pRS425	<i>2μ, Amp^R, LEU2</i>	[6]
pRS425-SUS1	<i>2μ, Amp^R, LEU2, SUS1-HA with 900 bp upstream and 700 bp downstream of UTR</i>	This study
pRS425-MEX67	<i>2μ, Amp^R, LEU2, MEX67-HA with 900 bp upstream and 700 bp downstream of UTR</i>	This study
pRS425-DBP5	<i>2μ, Amp^R, LEU2, DBP5-HA with 900 bp upstream and 700 bp downstream of UTR</i>	This study

Supplementary Table 3. Mean lifespans and P values for RLS analysis.

Figure	Strain	Strain description	Mean lifespan	P value compared to matched control strain
Figure 1A	BY4741	WT	27.3	control
	SY495	<i>sus1Δ</i>	20.2	0.0006, ***
	SY652	<i>sus1Δ</i>	22.8	0.0120, *
	SY653	<i>sus1Δ</i>	19.0	0.0001, ***
	SY654	<i>sus1Δ</i>	20.8	0.0009, ***
Figure 1C	BY4741	WT	19.2	control
	SY495	<i>sus1Δ</i>	13.8	0.0131, *
	FY231	<i>ubp8Δ</i>	31.9	<0.0001, ***
	FY399	<i>sgf11Δ</i>	23.8	0.3267, ns

	FY402	<i>sgf73Δ</i>	45.4	<0.0001, ***
	BY4741	WT	24.2	control
	SY495	<i>sus1Δ</i>	18.9	0.0002, ***
Figure 1D	FY390	<i>thp1Δ</i>	7.2	<0.0001, ***
	FY391	<i>sac3Δ</i>	9.3	<0.0001, ***
	FY451	<i>sem1Δ</i>	22.5	0.0623, ns
	BY4741	WT	23.7	control
Figure 2A	SY495	<i>sus1Δ</i>	17.2	<0.0001, ***
	FY231	<i>ubp8Δ</i>	31.6	0.0020, **
	SY786	<i>sus1Δ ubp8Δ</i>	18.8	0.0014, **
	BY4741	WT	21.9	control
Figure 2B	SY495	<i>sus1Δ</i>	17.0	0.0051, **
	FY399	<i>sgf11Δ</i>	26.3	0.0291, *
	SY787	<i>sus1Δ sgf11Δ</i>	19.1	0.2784, ns
	BY4741	WT	23.5	Control
Figure 2C	SY495	<i>sus1Δ</i>	17.1	<0.0001, ***
	FY402	<i>sgf73Δ</i>	40.4	<0.0001, ***
	SY797	<i>sus1Δ sgf73Δ</i>	23.5	0.3870, ns
	BY4741	WT	21.8	control
Figure 2D	SY495	<i>sus1Δ</i>	16.7	0.0028, **
	FY391	<i>sac3Δ</i>	8.5	<0.0001, ***
	SY784	<i>sus1Δ sac3Δ</i>	12.5	<0.0001, ***
	BY4741	WT	25.6	control
Figure 2E	SY495	<i>sus1Δ</i>	16.6	<0.0001, ***
	FY390	<i>thp1Δ</i>	5.7	<0.0001, ***
	SY1087	<i>sus1Δ thp1Δ</i>	5.1	<0.0001, ***
	BY4741	WT	24.2	control
Figure 2F	SY495	<i>sus1Δ</i>	18.6	<0.0001, ***
	FY451	<i>sem1Δ</i>	20.6	0.0188, *
	SY785	<i>sus1Δ sem1Δ</i>	10.5	<0.0001, ***
	BY4741	WT	29.7	<0.0001, ***
Figure 3A	SY529	<i>sir2Δ</i>	12.4	control
	SY557	<i>sir2Δ ubp8Δ</i>	11.9	0.2598, ns
	SY559	<i>sir2Δ sgf11Δ</i>	13.9	0.1020, ns
	SY558	<i>sir2Δ sgf73Δ</i>	13.8	0.8582, ns
	BY4741	WT	29.3	<0.0001, ***
Figure 3B	SY529	<i>sir2Δ</i>	8.8	control
	SY653	<i>sus1Δ</i>	20.4	0.0006, ***
	SY699	<i>sir2Δ sus1Δ</i>	11.0	0.0200, *
	BY4741	WT	23.7	<0.0001, ***
Figure 3C	SY529	<i>sir2Δ</i>	13.2	control
	SY556	<i>sir2Δ thp1Δ</i>	5.5	<0.0001, ***

	SY532	<i>sir2Δ sac3Δ</i>	5.6	<0.0001, ***
	BY4741	WT	23.9	control
Figure 4D	FY395	<i>MEX67-DAmP</i>	18.3	0.0007, ***
	FY396	<i>MTR2-DAmP</i>	20.8	0.0781, ns
	SY971	<i>sus1Δ</i> + pGP564	9.5	control
Figure 4E	SY972	<i>sus1Δ</i> + YGPM2h11 (<i>SUS1</i>)	28.3	<0.0001, ***
	SY973	<i>sus1Δ</i> + YGPM5d22 (<i>MEX67</i>)	16.1	<0.0001, ***
	SY974	<i>sus1Δ</i> + YGPM6e10 (<i>DBP5</i>)	24.8	<0.0001, ***
	SY1039	<i>sus1Δ</i> + pRS425	18.6	control
Figure 4G	SY1040	<i>sus1Δ</i> + pRS425- <i>SUS1</i>	25.8	<0.0001, ***
	SY1041	<i>sus1Δ</i> + pRS425- <i>MEX67</i>	23.7	0.0023, **
	SY1042	<i>sus1Δ</i> + pRS425- <i>DBP5</i>	21.7	0.0408, *

*** $P \leq 0.001$; ** $P \leq 0.01$; * $P \leq 0.05$; ns, not significant.

Supplementary References

- Ryu HY, Ahn S. Yeast histone H3 lysine 4 demethylase Jhd2 regulates mitotic rDNA condensation. *BMC Biol.* 2014; 12:75.
<https://doi.org/10.1186/s12915-014-0075-3>
PMID:25248920
- Longtine MS, McKenzie A 3rd, Demarini DJ, Shah NG, Wach A, Brachat A, Philippsen P, Pringle JR. Additional modules for versatile and economical PCR-based gene deletion and modification in *Saccharomyces cerevisiae*. *Yeast.* 1998; 14:953–61.
[https://doi.org/10.1002/\(SICI\)1097-0061\(199807\)14:10<953::AID-YEA293>3.0.CO;2-U](https://doi.org/10.1002/(SICI)1097-0061(199807)14:10<953::AID-YEA293>3.0.CO;2-U)
PMID:9717241
- Sung MK, Ha CW, Huh WK. A vector system for efficient and economical switching of C-terminal epitope tags in *Saccharomyces cerevisiae*. *Yeast.* 2008; 25:301–11.
<https://doi.org/10.1002/yea.1588>
PMID:18350525
- Jones GM, Stalker J, Humphray S, West A, Cox T, Rogers J, Dunham I, Prelich G. A systematic library for comprehensive overexpression screens in *Saccharomyces cerevisiae*. *Nat Methods.* 2008; 5:239–41.
<https://doi.org/10.1038/nmeth.1181>
PMID:18246075
- Sikorski RS, Hieter P. A system of shuttle vectors and yeast host strains designed for efficient manipulation of DNA in *Saccharomyces cerevisiae*. *Genetics.* 1989; 122:19–27.
<https://doi.org/10.1093/genetics/122.1.19>
PMID:2659436
- Christianson TW, Sikorski RS, Dante M, Shero JH, Hieter P. Multifunctional yeast high-copy-number shuttle vectors. *Gene.* 1992; 110:119–22.
[https://doi.org/10.1016/0378-1119\(92\)90454-w](https://doi.org/10.1016/0378-1119(92)90454-w)
PMID:1544568